University of New Orleans
ScholarWorks@UNO

University of New Orleans Theses and Dissertations | Dissertations and Theses

Fall 12-20-2017

One-way Coupled Hydroelastic Analysis of Aluminum Wedge Under Slamming

Mallikarjun Kalluru
University of New Orleans, New Orleans, mkalluru@uno.edu

Follow this and additional works at: https://scholarworks.uno.edu/td

 Part of the Other Engineering Commons

Recommended Citation

Kalluru, Mallikarjun, "One-way Coupled Hydroelastic Analysis of Aluminum Wedge Under Slamming" (2017). *University of New Orleans Theses and Dissertations*. 2414.
https://scholarworks.uno.edu/td/2414

This Thesis is protected by copyright and/or related rights. It has been brought to you by ScholarWorks@UNO with permission from the rights-holder(s). You are free to use this Thesis in any way that is permitted by the copyright and related rights legislation that applies to your use. For other uses you need to obtain permission from the rights-holder(s) directly, unless additional rights are indicated by a Creative Commons license in the record and/or on the work itself.

This Thesis has been accepted for inclusion in University of New Orleans Theses and Dissertations by an authorized administrator of ScholarWorks@UNO. For more information, please contact scholarworks@uno.edu.

One-way Coupled Hydroelastic Analysis of Aluminum Wedge Under Slamming

A Thesis

Submitted to the Graduate Faculty of the
University of New Orleans
in partial fulfillment towards the
requirements for the Degree of

Master of Science
in
Engineering
Naval Architecture and Marine Engineering

By

Mallikarjun Kalluru
B.E.-Naval Architecture and Offshore Engineering, 2012

December, 2017

Acknowledgement

I take this opportunity to thank all the people responsible in the sincerest manner possible for the completion of this thesis work.

I first thank my principal advisor Dr. Brandon M. Taravella, Associate Professor of Naval Architecture and Marine Engineering, University of New Orleans for providing me this opportunity to work under him to carry out this thesis work. There were multiple instances during this journey that his motivation and guidance helped me in breaking barriers and helping me complete this work.

I feel extremely grateful to my dear mates Mr. Lemuel Guedes Da Silva and Mr. Naresh Kumar Koyyappu for their support, solutions and suggestions that made this thesis bloom into fruition. I thank Mr. Naresh Kumar Koyyappu for letting me modify a couple of my subroutines from his parent subroutines INPUT and UDLAREA. I thank my dear mate Jonathan R. Eastridge for reviewing my thesis and providing me valuable suggestions.

I thank all my professors Dr. Lothar Birk, Dr. Brandon M. Taravella and Dr. Nikaloas Xiros for their tutelage in making my graduate studies a memorable and a fulfilling experience. I feel extremely grateful towards the Board of Regents (Grant # : LEQSF(2015-18)-RD-B-09) for supporting the research work on slamming that made this thesis work a possibility.

I thank my dear mates Mr. Vivek OS, Mr. Omar Jebari and Ms. Sushma Kalle for helping me both professionally and personally by offering me invaluable inputs during the course of my graduate studies and thesis work specifically.

Last but not the least I thank my family for their constant moral support and strength that they gave me during tough times which made me tackle the dire straits with a smile and hope.

Contents

List of Tables

List of Figures

Nomenclature

Z_{wl}	Wetted length without waverise
ν	Poisson's ratio
[K]	Stiffness Matrix
[C]	Damping Matrix
[M]	Mass Matrix
[A_m]	Added Mass Matrix
F	Force Vector
$\ddot{X}$	Acceleration Vector
$\dot{X}$	Velocity Vector
X	Displacement Vector
E	Youngs' Modulus
γ	Structural damping factor
ρ	Density of the plate
L	Length of the plate
B	Beam of the plate
β/γ	Newmark-beta coefficients
δ	Deflection of the plate

Abstract

The concept of using aluminum as the primary construction material for high speed ships and the hydroelastic behavior of the structure is widely gaining importance as a significant research topic in naval architecture. Aluminum is lighter than steel and hence can be predominantly used in high speed crafts which experiences significant slamming.

This thesis work is focused on wedge shaped models. Free fall wedge impact is studied and a FORTRAN 90 computer program is developed to estimate the structural response of the wedge experiencing slamming by the use of matrix methods, finite element techniques and Newmark-Beta numerical time integration methods.

The numerical solution is validated by comparison with the static solution. The theoretical hydrodynamic pressures which are used as input for this work was originally developed by using a flat cylinder theory [26]. The wedge drop at 0.6096 m (24 $inch$) drop height with an impact velocity of v=3.05 m/s is based as the premise and the experimental pressure distributions measured by the pressure-transducers and the theoretical pressure predictions are used as inputs and the structural response is derived.

Additionally, the response is compared for three different plate thicknesses and the results are compared against each other. The maximum deflection is comparable to the deflection evaluated from the experiment and tends to attain convergence as well. As the plate thickness reduces there tends to be a significant rise in the deflection values for the wedge plate, in the manner that when the plate thickness is halved there is a deviation of more than 75% in the deflection values as such.

Key words : Structural Response, Added mass, Plate element, Matrix methods, Finite Element Technique, Newmark-Beta Numerical Method, Slamming, Deflection

Chapter 1

INTRODUCTION

1.1 Slamming

Slamming in ship structures is an age-old topic spanning at least 82 years and is still of interest. The topic has still not yet been solved for a complete understanding; however, the work done until this point is exemplary nonetheless. The Classification Societies still consider the maximum bending moment is estimated as a factor for the dynamic effects and that slamming or whipping loads are still not yet soundly incorporated [10]. Numerous people from the academic, scientific and the research community have made significant strides and this thesis work just follows in the same footsteps.

Slamming can be expressed as sudden high hydrodynamic force resulting from accelerated pressures, impinging on the structure for a fleeting time instant which results in appreciable structural response. This happens when a body enters a fluid with a small relative angle between the body surface and free surface. In this case, the contact surface area between the fluid and the body expands at a high speed which gives rise to sudden acceleration of the fluid close to the interface, which results in high pressure.

Slamming is so critical that even mild slamming can introduce a whipping response of the ship's hull. During slamming, the fluid experiences high accelerations thereby creating a significant high-frequency contribution to the bending moment. This high frequency phenomenon leads to fatigue

induced stresses on the structure. The phenomenon of slamming is quite detrimental for the integrity of the ship's structure.

Slamming can have undesirable effects on the ship structure as it produces a huge impact force which acts repeatedly and impulsively and is usually oscillatory in nature. This is usually the case with a displacement craft where the bow of the ship rises and falls consequentially into the waves and because of the above said characteristics of the load the structure experiences failure.

The impact pressures depend heavily on the relative angle between the body and the fluid surface. From extensive research, experiments and the drop tests carried out it is understood that the pressure rises sharply for when the relative angle becomes small [10]. For relatively low deadrise angles it is found that the impact becomes more complex as air is being compressed in the phase before the impact. This high pressure region causes a depression of the fluid surface and allows the fluid to escape in the form of a jet at the ends of the body. This phenomenon actually gave a different insight to slamming as it was not just restricted to an impact but was also considered a planing phenomenon from then on as referenced from [12].

The slamming loads and its effects on the structure are investigated taking into consideration that the response to these loads are of hydroelastic nature, this phenomena also be expressed as fluid structure interactions. As the phenomenon of slamming is repeated and time-dependent it may lead to fatigue loads, hull whipping loads on the structure when exposed to long periods of time. It is not just restricted to fatigue loads, but because of the impulses involved, may lead to vibrational effects on the structure which is of transient nature.

1.2 Purpose and Motivation of the study

High speed crafts move by planing on the surface of water. This is possible because the boat trims by aft and the bow portion protrudes above the water surface. While traveling at high speeds, the fore end of the boat may experience slamming because of the frequency of wave encounter while

traveling in high seas.

The hull tends to deflect as the slamming pressures act on the hull. The deflection of hull plating changes the pressure gradient in a very complex manner which has undesirable effects on the structural response [10]. In order to solve an implicit equation of motion, the velocity or displacement vectors should be determined at an instant under impact loads. Then, the structural response of the hull can be estimated in consequential time instances.

As slamming is such a complex phenomenon, it has to be simplified into linear natured by assuming linearization and non-dimensionalities. The objective of this thesis is to develop a program to estimate the structural response of the plate panel experienced during one-way coupling by using the finite element method. Studies are performed to validate the stability and accuracy of the solution as well. The above said work is based on existing theories and concepts and these are explained thoroughly in the following chapter.

Overview

The 3D wedge hull is a homogeneous, prismatic planing hull of specific dimensions used for evaluating the structural behavior of the bottom plate during slamming. The 3D hull wedge entirely cannot be evaluated for deflections, hence the bottom plate panel is the one under consideration and that is to be evaluated for the structural behavior. The bottom plate panel is treated as a rectangular plate fixed-fixed across all the edges. The pressure distribution is variable across the breadth of the plate and considered constant across the length of the plate. There is a variation in the hydrodynamic loading because of the change in the wetted lengths as the section is immersed in the water. End effects are ignored for the purpose of this thesis work.

Scope

The scope of this thesis is to build, develop and validate a computer program to compute the transient structural response of the plate panel. The scope also includes comparison of the results derived from theoretical pressure prediction, experimental pressure prediction and the stereoscopic digital image correlation technique used for determining plate deflections. In addition, the scope of the thesis work includes the comparison between different plate thicknesses as well.

Chapter 2

LITERATURE REVIEW - EVOLUTION

Slamming has been investigated from various points of interest by using disparate methods for analysis such as the momentum theory, boundary element methods, statistical methods, analytical methods, computational fluid dynamics, structural aspects- hydroelasticity, experimental techniques, full scale measurements from the time it started with subsequent improvement in the results and the methods adopted.

The earliest work for understanding hydroelasticity was done by Bishop and Price in their publication [2] by investigation of the dry and wet elastic responses of the hull structure. This work serves as the beginning for understanding slamming.

2.1 Slamming - Momentum Approach

From a theoretical point of view, slamming loads have been mostly studied within the framework of potential flow theory, assuming blunt and rigid body and planar flow. The problem has been investigated from the impact approach since the beginning of the 20th century. The first investigations into the wave impact problem were made by Von Kármán [12] and Wagner [27] following which plenty of theories, publications and research have shaped the way the academic and the scientific community has responded to the slamming phenomenon.

Momentum theory [12] is the oldest theory to tackle the problem of slamming. The theory was initially applied to estimate the forces on the floats of the landing of sea planes. The forces acting on the planing hulls was first recognized as an impact problem in addition to the planing problem by Von Kármán in the National Advisory Committee for Aeronautics Technical Note No.321.

Von Kármán was the first to use the change in the added mass of the floats as an estimate of the impulsive force. He based the added mass of the sea plane float as that of a flat plate with finite width. The *planing problem was idealized as an impact problem*. The application of force on the planing hull was calculated by application of the momentum theory and the asymptotic solution.

The Von Kármán theory was developed based on the assumptions that the effects of gravity are neglected. The impact actually causes the fluid to accelerate thereby giving rise to added mass. The added mass is smaller than half of the apparent increase of mass owing to the wedge shaped bottom of the boat. As the plate wetting is considered only up to the waterline as a pioneering step the wetted length Z_{wl} is lesser than the wetted lengths as in the subsequent developments. The added mass and the impact loads are underestimated for small deadrise angles as the von Kármán's impact theory is based on momentum conservation.

The momentum approach was recently adopted by Kaspenburg and Thornhill [11] to calculate added-mass for a ship using a 3D panel at infinite frequency from which spatial added mass derivatives were developed. These added mass derivatives were multiplied by the relative velocity to find the impulsive force.

2.2 Slamming - Asymptotic Approach

Wagner [27] used potential flow theory to estimate the pressure distribution on wedges for understanding the constant velocity impact. His approach was mathematical and analytical. The impact of the float was linked to a planing hull thereby. The flow under the hull is idealized as equivalent to the flow around an expanding infinite flat plate with no chine. The impact pressures were

calculated by using modified Bernoulli's equation. The most significant feature to the solution of the impact problem of planing hulls was proposed by Wagner [27] when the jet rise-(the development of spray root) was incorporated in the estimation of the added mass, which was more accurate and realistic than that of the solution developed by Von Kármán.

The wetting factor $\pi/2$ is included as the theory proposed includes not just the waterline but the wave rise/spray root as well. This leads to interesting observations and results, which hold significance even today.

2.3 Slamming - Alternative Hydrodynamic Approach

Vorus [26] developed an alternative hydrodynamic theory for analysis of the slamming loads on the conventional hull sections operating in waves and the sections similar to the hydrodynamic planing hulls operating in calm waters. The new theory referenced by [26] is a hybrid method as it is considered a credible compromise between the asymptotic solutions pioneered by Herbert Wagner and the exact governing differential equations.

The impact pressures of slamming were well investigated by Vorus wherein the theory he developed approximates the geometry using linear approximations and performs the hydrodynamic analysis as a non-linear problem. Vorus proposed a boundary element method which takes a unified approach to the flow. The method proposed in this theory is a mixed theory. It is geometrically linear in the flat cylinder boundary conditions but it is hydrodynamically non-linear thereby fully retaining the large flow perturbation produced by the interacting cylinder in the axis boundary conditions.

2.4 Slamming - Analytical Approach

The analytical methods can help us reach the exact solution for a simplified impact problem. They serve to be the basis for the other tools such as boundary element methods to arrive at an appre-

ciable solution. Wagner pioneered in developing an analytical method for calculation of the impact problem solution.

The approximate solution for the free surface was refined by Dobroval'skaya [5] who developed an exact method for the similarity solution for the specific case of a wedge entering water vertically at a constant speed which dealt with impacting wedges. The solution is valid for any deadrise which has to be solved numerically proving to be an exact method for solving wedge impact problems.

Korobkin [13] also used Wagner's analysis with included higher order terms in the modified Bernoulli's equation in order to improve the quality of results of the theoretical predictions in comparison to the experimental results.

This method was extended to 3D applications by Scolan & Korokbin. A solution for axisymmetric bodies were found by their work. Cointe and Armand [1] studied the impact problem with an analytical approach where they considered the immersion depth must be comparable to the width of the section,which yielded very promising results.

2.5 Slamming - Hydroelastic Approach

Pabst [18] attempted to initially understand the structural behavior of the plate and investigated on making assumptions that the plate is stiff and that water is incompressible. His work proved that those assumptions weren't correct otherwise the structure should experience infinitely great forces thereby concluding that the plate has the property of elasticity. This lead to the fact that the seaplane floats could actually show different structural characteristics based on the boundary conditions of the plate. This showed the importance of flexible supports for the landing craft was.

Kvasvold and Faltinsen [9] reduced the problem of the plate with stiffeners to that of the flexible beam impacting on a wave crest in two dimensions. This beam was modeled as a Timoshenko beam and this was coupled to the simplified solution for the fluid flow in the impact region. An analytical solution was found but the work on numerical solutions (BEMs) failed for stability and convergence

reasons.

Kvalsvold, Faltinsen and Haugen [9] studied the local response induced because of slamming. This method is based on two dimensional analysis. Boundary element method was used and upon realization very large numerical errors were introduced. However, analytical based methods were used to calculate the slamming loads. The local slamming induced response was found to be governed by the relative impact velocity, the deadrise angle and the structural bending stiffness.

2.6 Slamming - Other Theoretical Approaches

It was well known that Wagner's solution had a singularity at the intersection between the body surface and the water surface. This singularity makes the solution very difficult to understand for a general shape of body. Yettou et al. [28] aimed at developing a better understanding of water loading and hull pressures experienced by a planing hull/wedge. Upon investigations, Yettou [28] found that the physical parameters such as drop height, deadrise angle and the weight actually influence the pressure distribution on the hull.

A method using strip theory was used to predict the slamming load which was developed by Carlos Guedes Soares [8] to determine the relative motion between the wedge/hull and the water surface and the rate of change in the momentum of the fluid to calculate the impact force. Timoshenko beam finite elements with a consistent mass formulation was implemented by the above investigator and the response was obtained using a Newmark integration scheme. The method proposed was an uncoupled solution combining Wagner theory and finite element analysis.

Zhao et al. [30] presented non-linear boundary element method to solve the water entry problem and verified the results with experimental drop tests of a wedge and a bow flare section. Zhao Rui and Faltinsen [30] studied the slamming load on hull cross-sections using a boundary element method and got an asymptotic solution for wetdeck slamming. The results from this were restricted by the limitation of the deadrise angle of the wedges. The results showed the importance of wave slope to

the slamming loads.

The results developed by the theories above said had been validated by numerous experiments conducted by Chuang [3], Fontaine and Cointe [7] in case of wedges, Cointe and Armand [1] in case of cylinders, Zhao et al., Maggie and Fontaine in case of realistic ship sections. The asymptotic solution from the theoretical prediction over predicts the max peak pressure.

Peseux [20] used finite element analysis technique to solve the impact problem in slamming which is of a non-linear nature. The experimental results were validated with the finite element analysis and were to be of an approvable value. Slamming loads are studied numerically wherein finite element analysis is used to solve the fluid domain. A coupling matrix between fluid and structure part is used to solve the hydroelastic impact problem as part of the method.

Different methods for fluid structure interactions have been developed by the academic and scientific community. Korobkin developed a theory to include the coupled equations to solve for the wedge impacts. A generalized Wagner theory is coupled with a finite element (FE) solution for the structure. Lu et al. [15] also presented a non-linear boundary element method for the water entry of the wedge and a finite element technique is applied for the coupled,structural response.

Datta [4] developed a method to provide the dynamic response spectra to study the transient fluid-structure dynamics representative of impact loads and slamming pressures. The plate deflections were derived both in space and time by modeling the plate as a beam and then implementing the time integration 4th order Runge-Kutta technique and Galerkin methods for finite elements. The study also includes the structural response with respect to various physical parameters such as aspect ratio, damping ratio, boundary conditions and deadrise.

Panciroli et al. [19] presented a fully coupled solution for a hydroelastic entering water by applying the smooth particle hydrodynamics method with a finite element code. Piro and Maki [21] implemented a modified Reynolds Average Navier Stokes formulation for the water entry of the wedge, coupled with a finite element analysis technique.

Jian Lv and Grenetstedt [16] developed a theory in which the deformation of the boat hull during the slamming phenomenon is studied analytically by using a Euler-Bernoulli beam as a representation of the bottom panel of the boat. Koyyappu developed a numerical tool for calculating and estimating the 2 dimensional wedge deflection in his thesis work at the University of New Orleans, Fall 2016 [14]. The current work is an extension to that.

Eastridge measured the bottom plate deflection by conducting wedge-drop experiments,using strain gauges and stereoscopic digital image correlation technique and compared the results between those in his work [6] which acted as a precursor for the comparison performed in this thesis work. The above said references provide the necessary background upon which the following thesis has been developed.

The fixed-fixed end condition of the bottom wedge plate panel is taken into account and hydrodynamic loads are applied on the wetted nodes along the breadth of the plate panel. This is explained in detail in Chapter 4. The slamming pressures are impulsive and act for a fleeting time instant. The response to this forces can be generated by developing a numerical code to calculate the deflection of the plate panel. The methodology used for developing the code is presented in Chapter 4. The numerical method used for the code has been validated by means of static solutions in Chapter 6 and the results are discussed in Chapter 7. Ultimately, the conclusions and future work are presented in Chapter 8 to give a comprehensive understanding.

Chapter 3

BACKGROUND

The slender planing 3D aluminum wedge model is built to perform wedge-drop slamming experiments to understand the structural response of the bottom panel to slamming. An insight into the 3D wedge model, the problem and the background work for the same is presented in this chapter. The assumptions and simplifications are explained here.

3.1 Wedge Model

An aluminum wedge hull of constant cross section with the following principal particulars is considered. Simplifications and idealizations are made in order to calculate the deflection of the plate which ensues further into the thesis. The transverse view and the boundary conditions of the wedge follows later for better understanding. The wedge has the following dimensions and particulars:

Parameter	Value	Unit
Length of the wedge	1.450	m
Beam of the wedge	0.600	m
Depth of the wedge	0.5334	m
Density of aluminum	2700	kg/m^3
Thickness of the bottom plate	0.00635	m
Thickness of the side plate	0.00375	m
Damping factor of aluminum	0.002	
Modulus of elasticity of aluminum	69x10^9	N/m^2
The weight of the wedge	1153.60	N/m
Poisson's ratio of aluminum	0.33	
Dead rise angle	20	deg

Table 3.1: Wedge Particulars

The transverse section of the wedge is shown below:

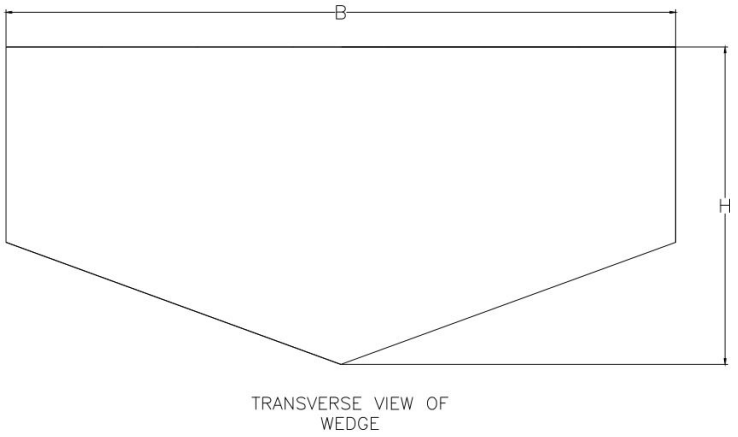

Figure 3.1: Transverse view of the wedge

3.2 Boundary Condition

As the slamming impact is very significant on the bottom plating of the model when compared to the sides, the bottom plating of the highly complex 3-D wedge model is simplified to a rectangular plate for the purpose of this thesis. The area of interest is not the whole model of the wedge however

it is only the bottom plate that is under consideration. The bottom panel is considered as a flat plate, and the hydrodynamic loading occurs on the flat plate. The nature of the hydrodynamic loading is impulsive. The fixed-fixed end conditions for the flat plate is shown in figure 3.2 below.

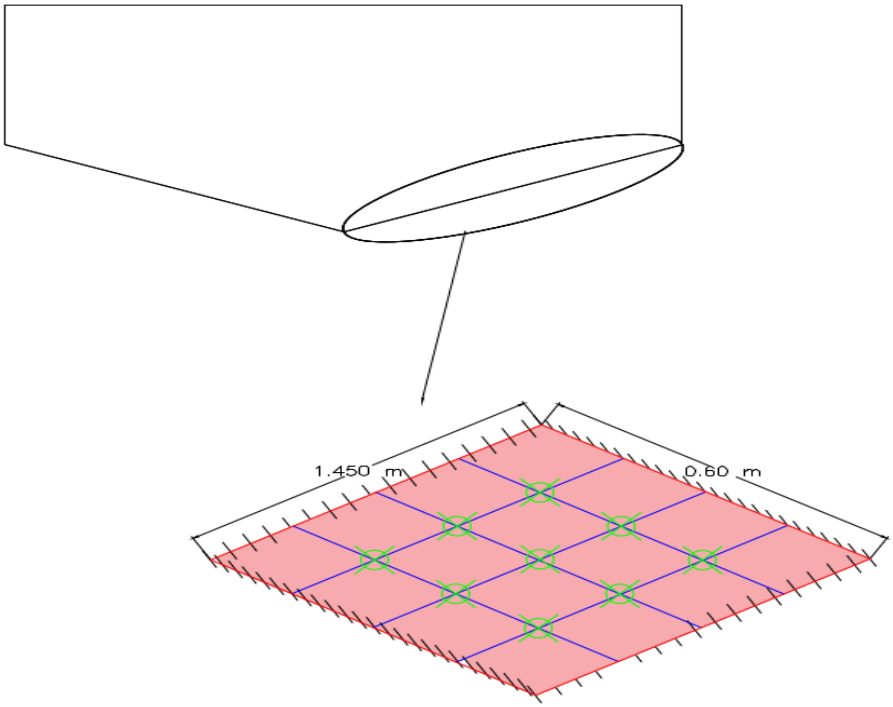

Figure 3.2: Wedge plate - Fixed-fixed boundary conditions

3.3 Governing Equation

Each structural finite element problem is defined by stiffness[K], mass[M] and damping[C]. These parameters are imparted to the finite elements which actually make it suitable to be solved by the ordinary differential equation $m\ddot{x} + c\dot{x} + kx = f(t)$ as a function of time.

Each physical process is governed by an equation to understand the engineering sense behind

it. As the process is dynamic here and is time dependent the process can be explained by basing it on the classical ordinary differential equation of mechanical vibration as explained below:

$$[M(t)]\{\ddot{X}(t)\} + [C]\{\dot{X}(t)\} + [K]\{X(t)\} = F\{t\} \tag{3.1}$$

where,

- [K] - Stiffness matrices of each finite element of the bottom plate (size - degrees of freedom x degrees of freedom)
- [C] - Structural damping matrices of the finite elements (size - degrees of freedom x degrees of freedom)
- [M] - The total mass matrix of the plate upon wedge drop which is the sum of the mass matrices and the hydrodynamic added mass matrices of the finite elements concentrated at the nodes. (size - degrees of freedom x degrees of freedom)
- F - Force vector which includes the forces and the moments terms alternatively in the force vector. (size - degrees of freedom x 1)
- $\ddot{X}$ - Acceleration vector (size - degrees of freedom x 1)
- $\dot{X}$ - Velocity vector (size - degrees of freedom x 1)
- X - Displacement vector (size - degrees of freedom x 1)

The solution of the above said time-dependent dynamic equation can be obtained by solving the equation 3.1 by means of a time stepping technique where the stiffness matrix [K] of size(degree of freedom x degree of freedom), damping matrix [C] of size(degree of freedom x degree of freedom), mass matrix [M(t)] of size(degree of freedom x degree of freedom) and the force vector $\{F\}$ of size

(degree of freedom x 1) is passed as inputs to the time stepping technique and the displacement $\{\mathrm{X}\}$, velocity $\{\dot{X}\}$ and the acceleration $\{\ddot{X}\}$ is found as a result of that at each defined time step. The process of solving this equation using the explicit time-stepping numerical method is extensively written in the following chapter.

Chapter 4

METHODOLOGY

Hull slamming and planing is widely regarded as an impact problem for wedge shaped structures. As explained in the previous sections, it is understood that the structure experiences a very high magnitude excitation force for a very short interval of time. The structural response experienced is transient in nature as it involves loads as a function of time. This kind of a response is called as transient response. The hydrodynamic pressure distribution varies non-linearly in both space and time. This response is dependent on the initial conditions and the response is solved using the stable time stepping Newmark-Beta method in the following thesis work [17].

4.1 Physical Methodology

Stiffness is the rigidity of an object to resist deformation and this property for the plate panel is represented by the pre-defined stiffness matrix as referred from [23]. The local stiffness matrix that is used for this purpose is explained in Chapter 5. The stiffness matrix has to be developed for the whole plate by assembling elemental stiffness matrices. The mass is represented by the mass matrix and that the mass is not static and the matrix keeps changing with each time step as the wetted length keeps changing. These above said matrices are built to form the equation 3.1.

In order to solve the equation, the right hand side force vector is actually developed from the

variable pressure distribution that is fed into the equation. As it is a time dependent process, the equation has to be solved by making use of the implicit numerical method as in this case the Newmark-Beta numerical method. This is used for solving the system of equations at each time step thereby finding out the unknowns displacement, velocity and acceleration at each time step.

4.2 Local Stiffness Matrix

The selected local stiffness matrix as referred from [23]. The elemental stiffness matrix is built

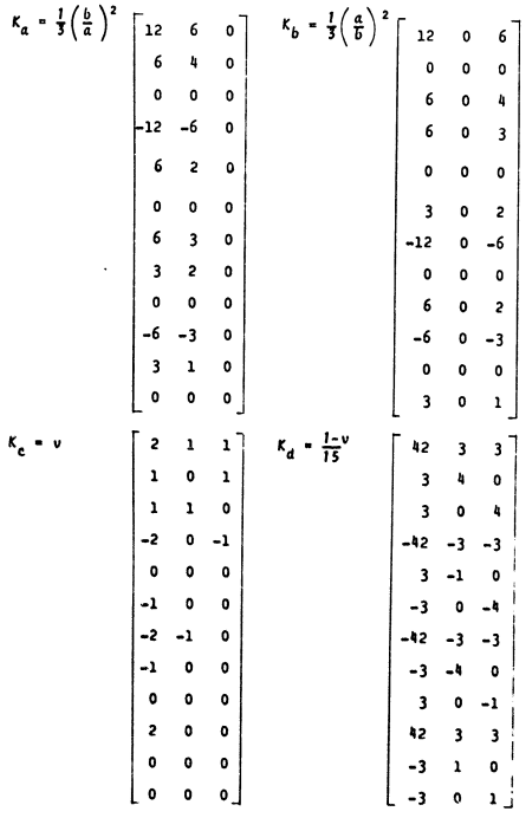

Figure 4.1: Individual stiffness matrices - [K$_a$], [K$_b$], [K$_c$], [K$_d$] (Ian.R.Stubbs, 1966)

up from four individual matrices K$_a$,K$_b$,K$_c$ and K$_d$ as shown in figure 4.1. The sum of these individual stiffness matrices actually give rise to the individual submatrix K$_i$ which arranged to form the 12x12

local stiffness matrix [K] as shown in figure 4.2.

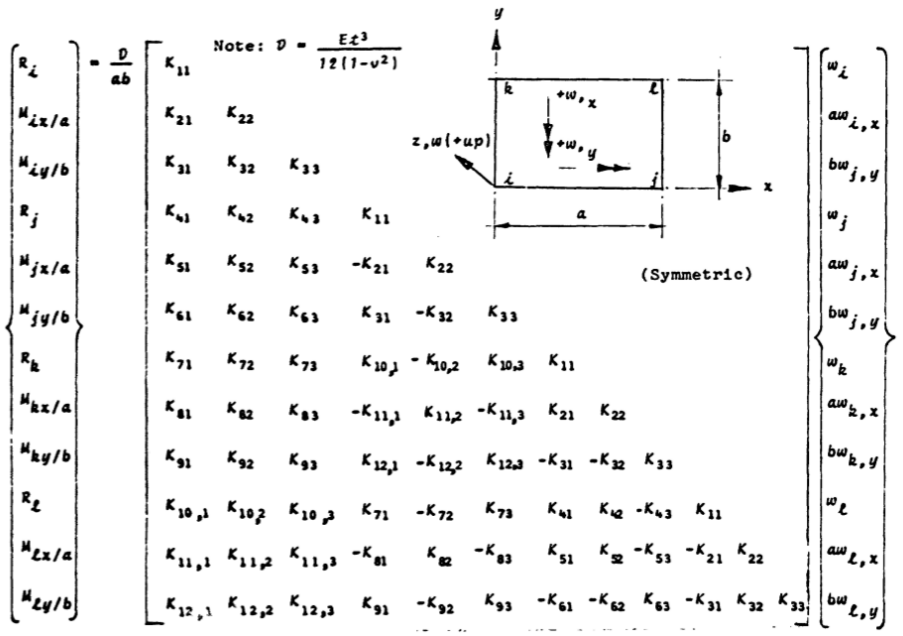

Figure 4.2: The Local Stiffness Matrix based on dynamic response of blasts for box-type structures

4.3 Development of Matrices

Stiffness and Damping Matrices

Each matrix that constitutes the governing equation has a distinctive structure of its own. All the matrices share a common thread that all are diagonally symmetric in nature. The elemental stiffness matrix of a plate element is of size 12×12. It is very cumbersome to build a stiffness matrix for the plate element and quite advisable to make use of the previously developed matrices by the scientists and engineers all around until now. Upon trials and tribulations it was found that the stiffness matrix for the Adini-Clough element [23] was the most suitable for this case like a dynamic process. The stiffness matrix is diagonally symmetrical and represented as below:

Elemental Stiffness Matrix:

$$[K_{12x12}] = \begin{bmatrix} K_{11} & & & & & & \\ K_{21} & K_{22} & & & & & \\ K_{31} & K_{32} & K_{33} & & & & \\ K_{41} & K_{42} & K_{43} & K_{11} & & & \\ \vdots & \vdots & \vdots & \vdots & \ddots & & \\ \vdots & \vdots & \vdots & \vdots & \dots & \ddots & \\ \vdots & \vdots & \vdots & \vdots & \dots & \dots & K_{33} \end{bmatrix} \tag{4.1}$$

This local stiffness matrix is intuitively assembled to develop the global stiffness matrix for the whole plate with the matrix size depending upon the number of elements discretized. The size of the matrix size would be (N+1)×(N+1)×3 which is actually the number of degrees of freedom of the plate where actually N represents the number of elements for the mesh. Each plate node has three degrees of freedom with one linear and two rotational degrees of freedom. The generic plate element is shown in figure 4.3.

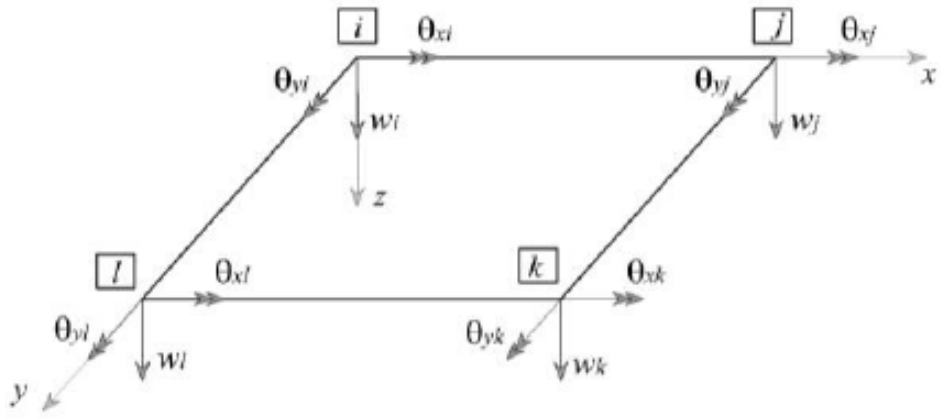

Figure 4.3: Rectangular plate element with three degrees of freedom at each plate node

The structural damping matrix [C] is an extension to the stiffness matrix in the sense that it is developed by taking the product of the damping factor to the global stiffness matrix [K]. The damping factor is multiplied with each and every term in the global stiffness matrix to develop the global damping matrix [C].

4.3.1 Global Stiffness Matrix

The bottom plate panel is discretized arbitrarily into 4 noded rectangular elements. Each node for the element has 3 degrees of freedom, which results in the local stiffness, damping and mass matrices to be of 12×12 sizes.

The elemental 12×12 stiffness matrix for a rectangular element is essentially linked to the plate by making use of the connectivity matrix which results from the CONNECTIVITY SUBROUTINE in the case of the program. Initially, connectivity matrices are formed which relate the local to the global system. An example is cited below to understand the method in a better manner.

Consider the bottom plate panel to be arbitrarily discretized into 2x2 elements (totally 4 rectangular elements). For this arbitrary discretization the degree of freedom for the plate is computed to be 27 degrees of freedom, thereby the connectivity matrix(dof,12) is of size Bmat(27,12). The connectivity matrix is built up as follows. The quasi-global [Kq] matrix is developed from the :

$$\begin{bmatrix} 1 & 0 & \dots & \dots & \dots & \dots & 0 \\ 0 & 1 & 0 & \dots & \dots & \dots & 0 \\ 0 & 0 & 1 & 0 & \dots & \dots & 0 \\ 0 & 0 & 0 & B_{MAT} & 0 & \dots & 0 \\ 0 & 0 & 0 & (27\times 12) & \ddots & 0 & 0 \\ \vdots & \vdots & \vdots & \vdots & \ddots & \vdots & \vdots \\ 0 & 0 & 0 & 0 & \dots & \dots & 0 \\ 0 & 0 & 0 & 0 & \dots & \dots & 0 \\ 0 & 0 & 0 & 0 & \dots & \dots & 0 \end{bmatrix} \times \begin{bmatrix} k_{1,1} & k_{1,2} & k_{1,3} & \dots & \dots & k_{1,12} \\ k_{2,1} & k_{2,2} & k_{2,3} & \dots & \dots & k_{2,12} \\ k_{3,1} & k_{3,2} & k_{3,3} & \dots & \dots & k_{3,12} \\ k_{4,1} & k_{4,2} & k_{4,3} & Local-k & \dots & k_{4,12} \\ k_{5,1} & k_{5,2} & k_{5,3} & (12\times 12) & \ddots & k_{5,12} \\ \vdots & \vdots & \vdots & \vdots & \ddots & \vdots \\ k_{10,1} & k_{10,2} & k_{10,3} & \dots & \ddots & k_{10,12} \\ k_{11,1} & k_{11,2} & k_{11,3} & \dots & \dots & k_{11,12} \\ k_{12,1} & k_{12,2} & k_{12,3} & \dots & \dots & k_{12,12} \end{bmatrix} = \begin{bmatrix} \\ \\ \\ \\ K_q - QuasiGlobal \\ (27\times 12) \\ \\ \\ \\ \end{bmatrix}$$

$$\underset{27\times12}{[B_{MAT}]} \times \underset{12\times12}{[Elemental-k]} = \underset{27\times12}{[K_q]} \tag{4.2}$$

The quasi-global matrix shall be converted to the global matrix by multiplying the quasi-global matrix with the transpose of the connectivity matrix.

$$\begin{bmatrix} \\ \\ \\ \\ \\ \\ \\ \\ \\ \\ \\ \\ \\ \\ \end{bmatrix}_{\substack{K_q - QuasiGlobal \\ (27\times12)}} \times \begin{bmatrix} 1 & 0 & \dots & \dots & \dots & \dots & 0 \\ 0 & 1 & 0 & \dots & \dots & \dots & 0 \\ 0 & 0 & 1 & 0 & \dots & \dots & 0 \\ 0 & 0 & 0 & {B_{MAT}}^T & 0 & \dots & 0 \\ 0 & 0 & 0 & (12\times27) & \ddots & 0 & 0 \\ \vdots & \vdots & \vdots & \vdots & \ddots & \vdots & \vdots \\ 0 & 0 & 0 & 0 & \dots & \dots & 0 \\ 0 & 0 & 0 & 0 & \dots & \dots & 0 \\ 0 & 0 & 0 & 0 & \dots & \dots & 0 \end{bmatrix} = \begin{bmatrix} \\ \\ \\ \\ \\ \\ \\ \\ \\ \\ \\ \\ \\ \\ \end{bmatrix}_{\substack{K-GlobalStiffness \\ (27\times27)}}$$

$$\underset{27\times12}{[K_q]} \times \underset{12\times27}{[B_{MAT}]^T} = \underset{27\times27}{[K]} \tag{4.3}$$

The global matrix developed as a result of this is the global stiffness matrix based on one discretized plate element. As discussed earlier, N x N number of global stiffness matrices shall be developed and all these global matrices are assembled to form the final global matrix [K] as shown in equation 4.4

$$[K_{total}] = \sum_{i=1}^{N} [K_i] \tag{4.4}$$

Mass and addedmass matrix

A matrix of size 12x12 is built to describe the elemental mass matrix. As discussed earlier, the local mass matrix is combined together and summed up which results in a global mass matrix of the size degree of freedom x degree of freedom.

Elemental Mass Matrix:

$$[M_{12x12}] = \begin{bmatrix} M_{xx} & & & & & & \\ 0 & I_{yz} & & & & & \\ 0 & 0 & I_{zx} & & & & \\ 0 & 0 & 0 & M_{yy} & & & \\ \vdots & \vdots & \vdots & \vdots & \ddots & & \\ \vdots & \vdots & \vdots & \vdots & \dots & \ddots & \\ \vdots & \vdots & \vdots & \vdots & \dots & \dots & I_{xy} \end{bmatrix} \tag{4.5}$$

There is an inertial component added to the highly accelerating wedge as some volume of fluid is displaced when the process is carried out through a range of time steps. This hydrodynamic mass matrix is added to the already static mass matrix thereby resulting in the final mass matrix for each individual time step. This apparent mass is called the added mass which is computed at each independent time step based on the wetted length of the wedge and this added mass is added to that particular static mass thereby resulting in the total mass matrix ie. [M]+$[A_m]$ = Total Mass Matrix.

4.3.2 Mass Global Matrix

This section includes the manner in which the final mass global matrix is developed for the bottom plate panel for the same case as discussed in sec 4.3.1. The quasi-global mass matrix is as follows.

$$\begin{bmatrix} 1 & 0 & \dots & \dots & \dots & \dots & 0 \\ 0 & 1 & 0 & \dots & \dots & \dots & 0 \\ 0 & 0 & 1 & 0 & \dots & \dots & 0 \\ 0 & 0 & 0 & B_{MAT} & 0 & \dots & 0 \\ 0 & 0 & 0 & (27 \times 12) & \ddots & 0 & 0 \\ \vdots & \vdots & \vdots & \vdots & \ddots & \vdots & \vdots \\ 0 & 0 & 0 & 0 & \dots & \dots & 0 \\ 0 & 0 & 0 & 0 & \dots & \dots & 0 \\ 0 & 0 & 0 & 0 & \dots & \dots & 0 \end{bmatrix} \times \begin{bmatrix} M_{1,1} & 0 & 0 & \dots & \dots & \dots & 0 \\ 0 & M_{2,2} & 0 & \dots & \dots & \dots & 0 \\ 0 & k_0 & M_{3,3} & \dots & \dots & \dots & 0 \\ 0 & 0 & 0 & M_{4,4} & Local - Mass & \dots & 0 \\ 0 & 0 & 0 & 0 & (12 \times 12) & \ddots & 0 \\ \vdots & \vdots & \vdots & \vdots & \ddots & \vdots & \vdots \\ 0 & 0 & 0 & \dots & M_{10,10} & 0 & 0 \\ 0 & 0 & 0 & \dots & \dots & M_{11,11} & 0 \\ 0 & 0 & 0 & \dots & \dots & \dots & M_{12,12} \end{bmatrix} = \begin{bmatrix} \\ \\ \\ \\ M_q - QuasiGlobal \\ (27 \times 12) \\ \\ \\ \\ \\ \end{bmatrix}$$

$$\underset{27\times12}{[B_{MAT}]} \times \underset{12\times12}{[Elemental - M]} = \underset{27\times12}{[M_q]} \tag{4.6}$$

The quasi-global matrix shall be converted to the global matrix by multiplying the quasi-global matrix with the transpose of the connectivity matrix.

$$\begin{bmatrix} \\ \\ \\ \\ M_q - QuasiGlobal \\ (27 \times 12) \\ \\ \\ \\ \\ \end{bmatrix} \times \begin{bmatrix} 1 & 0 & \dots & \dots & \dots & \dots & 0 \\ 0 & 1 & 0 & \dots & \dots & \dots & 0 \\ 0 & 0 & 1 & 0 & \dots & \dots & 0 \\ 0 & 0 & 0 & {B_{MAT}}^T & 0 & \dots & 0 \\ 0 & 0 & 0 & (12 \times 27) & \ddots & 0 & 0 \\ \vdots & \vdots & \vdots & \vdots & \ddots & \vdots & \vdots \\ 0 & 0 & 0 & 0 & \dots & \dots & 0 \\ 0 & 0 & 0 & 0 & \dots & \dots & 0 \\ 0 & 0 & 0 & 0 & \dots & \dots & 0 \end{bmatrix} = \begin{bmatrix} \\ \\ \\ \\ M - GlobalMass \\ (27 \times 27) \\ \\ \\ \\ \\ \end{bmatrix}$$

$$\underset{27\times12}{[M_q]} \times \underset{12\times27}{[B_{MAT}]^T} = \underset{27\times27}{[M]} \tag{4.7}$$

The global matrix developed as a result of this is the global mass matrix based on one discretized plate element. As discussed earlier, N x N number of global mass matrices shall be developed and all these global matrices are assembled to form the final global matrix [M] as shown in equation 4.5.

$$[M_{total}] = \sum_{i=1}^{N} [M_i] \tag{4.8}$$

4.4 Program - Building Blocks

The program begins with the principal parameters of the hull as inputs followed by which the arbitrary number of mesh elements is specified. This in turn leads to finding out the matrix sizes and building them accordingly based on the arbitrary number of elements. The program is built in a manner that the [K], [C] and [M] matrices for the local element is written down as local 12×12 matrix based on the discretized rectangular plate element. These matrices are combined together by the principle of finite element analysis to develop the large global matrix based on the arbitrary number of the elements.

Consequentially, the hydrodynamic pressures are read from an output file, generated by an external hydrodynamic code developed for [25]. These pressures are integrated over the plate surface to find the external excitation forces at the arbitrary locations. These excitation forces are resolved into the nodal reactions and distributed across all the nodes of the plate. Finite element analysis requires the nodal forces to be evaluated which are done subsequently.

However, as the process is dynamic and that added mass keeps changing hence the above said ordinary differential equation needs to be solved by developing the total mass matrix. This is done by updating the added mass matrix at each time instant and summed up with the static mass matrix at each instant. This equation 3.1 is solved by a time stepping method thereby yielding deflection,velocity and acceleration of the plate nodes.

4.5 Finite Element Modeling

The bottom plate is discretized into arbitrary number of elements based on the accuracy and the convergence of the solution.The rectangular plate is a member which has homogeneous physical parameters such as mass,stiffness and damping acting throughout the member. Each node is considered to have 3 degrees of freedom, for a plate having mesh size N$\times$N, the number of nodes would be

(N+1)x(N+1) or if the plate has mesh size then can be adjusted accordingly and the size of [K], [C] and [M] matrices would be [K/C/M] = ((N+1)×(N+1))×3 according to the degrees of freedom. The mesh size is not restricted only to N×N, but M×N is applicable as well.

4.6 FORTRAN PROGRAM - OVERVIEW

This section describes the working procedure of the code in a very coherent and conclusive manner.

- The following input parameters for the wedge hull are initialized and declared which include the dimensions of the plate *L and B* , Poisson's ratio ν, Damping Coefficient γ and Young's Modulus *E*.
- It has to be noted that all the matrices and vectors are of dynamic allocation.
- The stiffness matrix for the plate is formulated based on the above said.
- A rectangular plate element has four nodes and each node has three degrees of freedom which leads to developing a local stiffness matrix of size 12x12 (4 nodes x 3 degrees of freedom).
- The process for developing a stiffness matrix of size 12x12, is not regular as in the case of the beam and hence Adini-Clough plate element stiffness matrix which has greater suitability to time stepping methods had to be programmed.
- The SUBROUTINE 'STIFFELE' is the one in which the 12x12 local stiffness matrix for a plate element is defined.
- The local stiffness matrix can be converted into the global stiffness matrix by making use of the subroutine 'CONNECTIVITY'. This actually combines the local stiffness matrices to develop a global matrix based on the arbitrary size of the degree of freedom based on the mesh size.

– The local damping matrix for the plate is developed along with the local mass matrix for the plate and as discussed earlier the matrices are developed globally by using the 'CONNECTIVITY' SUBROUTINE.

– At this stage the global matrices of stiffness matrix [K],damping matrix [C] and the mass matrix [M] is developed.

– The three matrices are of the sizes degree of freedom x degree of freedom however, based on the nature of the plate restraints it has to be recognized that these matrices need to be reduced in size only to the number of the remaining degrees of freedom as against the restrained nodes and its degrees of freedom.

– Hence, the matrices are reduced in size arbitrarily based on the boundary conditions.

– The force vector to solve the equation of motion is developed from the input hydrocode where the hydrodynamic pressures for the wedge plate are integrated numerically through each time instant thereby yielding a force vector at each time instant (ts).

– The total force vector at each time instant needs to be distributed across the nodes on the arbitrarily sized finite element mesh. The above said force vector is developed by making use of the 'INPUT' SUBROUTINE.

– As the wedge drop is a dynamic process the drop tends to lead to the fluid particles being accelerated under the action of the drop thereby giving rise to the concept of added masses which acts on the bottom surface of the hull.

– The fluid particles under acceleration/deceleration imparts a virtual mass to the body as the body moves through the volume of the fluid around it.

– The added mass is computed by using the empirical formula and in this programming model it is computed by using the 'UDLAREA' SUBROUTINE.

– These added mass needs to be added to the original mass matrix of the plate there by giving rise to the final mass matrix [M_{final}] = [M] + [ΔM].

– The added mass matrix is dynamic in nature as well and needs to be updated for each time step in a specific time interval.

– Now all the matrices for the time stepping technique have been formulated and the equation is ready to be solved with the time stepping technique.

– The transient response of the plate can be computed by using the 'NEWMARK' SUBROUTINE where the deflections,velocities and the accelerations of the plate at each and every node can be calculated. This gives us the structural behaviour of the plate dynamically through each timestep.

– The flowchart for the entire working program is shown subsequently.

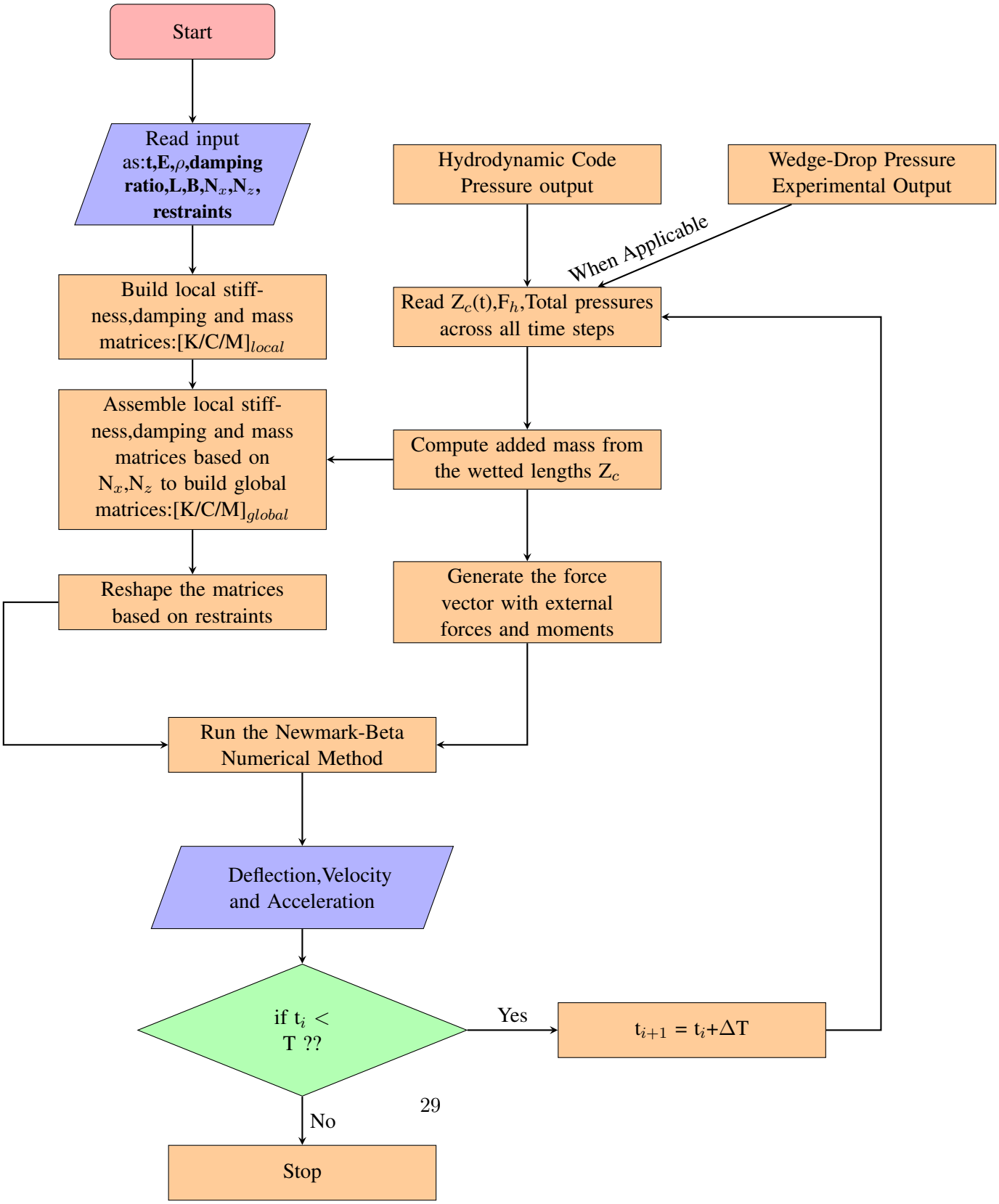
Start
Read input as:t,E,ρ,damping ratio,L,B,N$_x$,N$_z$, restraints
Build local stiffness,damping and mass matrices:[K/C/M]$_{local}$
Assemble local stiffness,damping and mass matrices based on N$_x$,N$_z$ to build global matrices:[K/C/M]$_{global}$
Reshape the matrices based on restraints
Hydrodynamic Code Pressure output
Wedge-Drop Pressure Experimental Output
When Applicable
Read Z$_c$(t),F$_h$,Total pressures across all time steps
Compute added mass from the wetted lengths Z$_c$
Generate the force vector with external forces and moments
Run the Newmark-Beta Numerical Method
Deflection,Velocity and Acceleration
if t$_i$ < T ??
Yes
t$_{i+1}$ = t$_i$+ΔT
No
Stop

4.7 Wedge impact - flow physics

The hydrodynamic model obeys the laws of potential flow physics thereby rendering it to be incompressible, irrotational and inviscid. Gravity is neglected as well in understanding the flow physics. An impacting flat cylinder model is considered for investigation and the hydrodynamic solution is developed for the same wherein the cylinder model actually experiences complete penetration i.e. chine wetted flow into the water surface as shown below.

The point where there is a discontinuity in the hull structure, termed as chine is the point where the flow tends to separate in most cases unless and until there is a premature separation attributing to some other cause. In case of premature separation, there would be no further advance of the point at which the flow contour has zero pressure. The theory is built on the assumption of the symmetry about the Y-axis, the vertical plane of the cylinder.

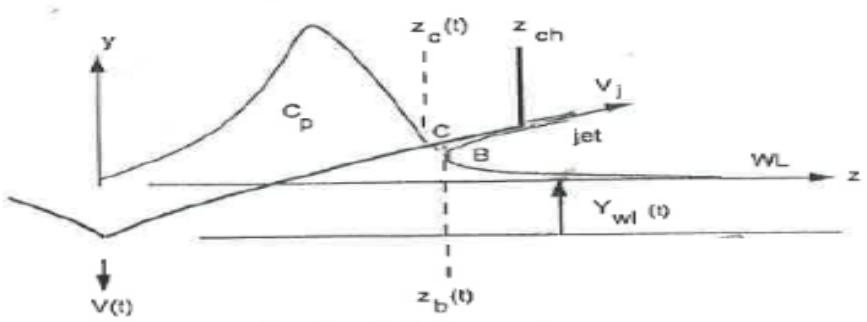

Figure 4.4: (a) Cylinder impact - Chine Unwetted Flow(Vorus,1996)

Upon the cylinder impacting against the free surface, it is found that the free surface returns back forming a jet in the beginning of the impact as shown in figure 4.4(a). The 'spray root' rapidly advances along the cylinder profile followed by point C. It is realized that the contour pressure be-

comes zero at pt. C and beyond. Point C keeps on moving outward till it reaches the chine.

Initially there is a point B past point C and this as well continues to advance further outward than the chine leaving behind point C. Point C is where the last pressure point in the pressure distribution acts whereas the point B lies outside of this pressure distribution.

Point C is the point where the flow detaches itself from the cylinder profile as shown in figure 4.5(b). On the region of fluid flow indicated by B the flow velocity is higher than the impact velocity where as in the lower region the flow velocity is lower than the impact velocity.

For analysis, the cylinder is collapsed onto the z-axis. The interesting character of the flow is that the tangential velocity drops in the region $Z_c <= Z <= Z_b$ by an order of magnitude on the flow becoming a chine wetted flow.

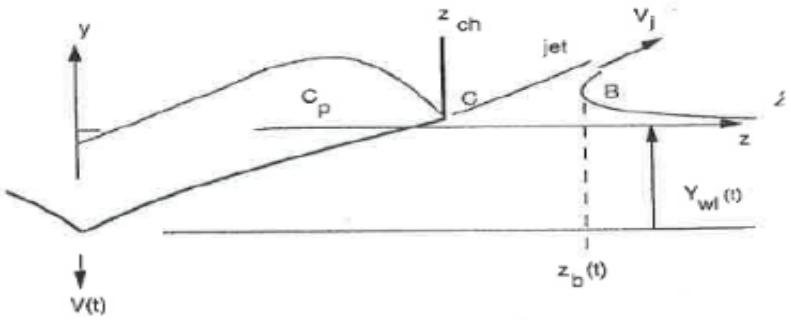

Figure 4.5: (b) Cylinder Impact-Chine Wetted Flow (Vorus,1996)

4.8 Pressure Distributions to Forces and Moments

The pressure distribution referenced from the output of the theoretical pressure prediction hydrodynamic code written for [25], is made use of to convert the pressures into nodal forces and moments to make use of in the application for the finite element technique.

4.8.1 Theoretical Pressure Distribution

The theoretical pressure distribution varies impulsively on the wedge plate and it is shown as below:

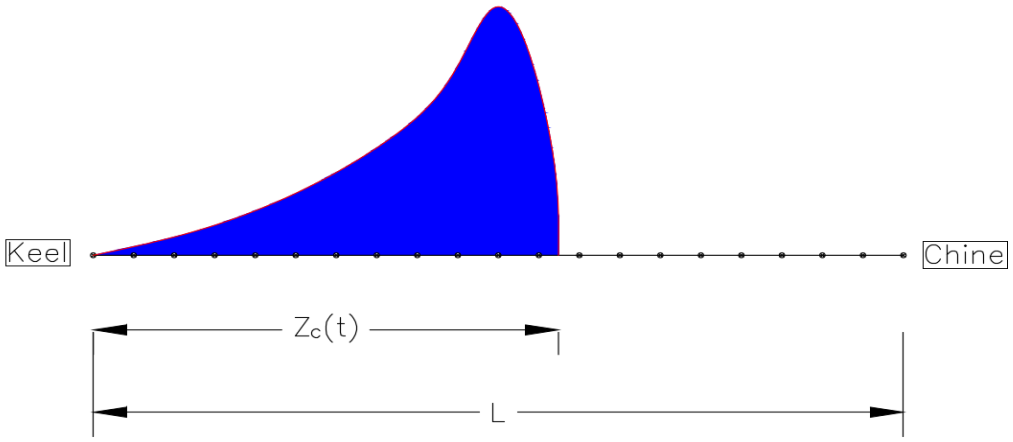

Figure 4.6: Variable Pressure distribution on the bottom plate

As already stated, the program works in such a manner that the pressure distribution evaluated over a fixed number of discretizations for the wedge plate needs to be suitably juxtaposed in correspondence with the arbitrary number of discretizations.

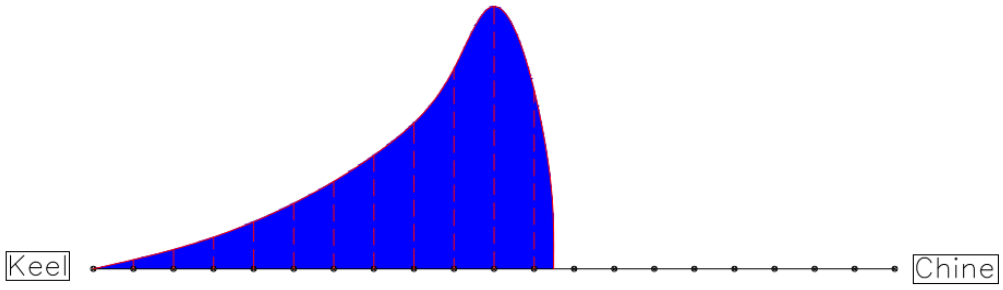

Figure 4.7: Pressure distribution evaluated over discretized elements

These pressure distributions at each time instant are integrated over the breadth and that the

force per unit length is calculated. For all simplification this case has been discussed only as a beam as shown below, but in reality the pressure distribution is across the rectangular bottom plate where the pressure distribution in the other axis is considered can be interpreted as uniformly loaded distribution. For all practical purposes, in the scope of this thesis work the 3D flow effects shall be neglected. The

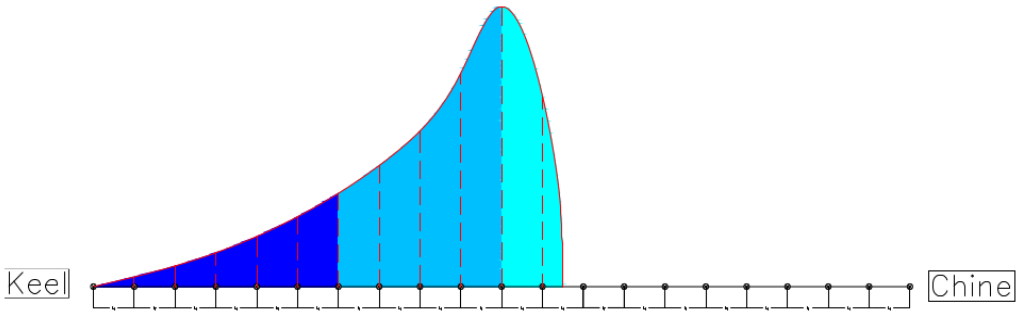

Figure 4.8: Integration of pressure distribution across the side of the bottom plate

conversion of the pressure distributions to the nodal forces and moments requires the integration of the force/length uniform distribution across the other axis of the rectangular plate. This is done by taking the product of the elemental length and the force/length distribution at each time step and across all distributions.

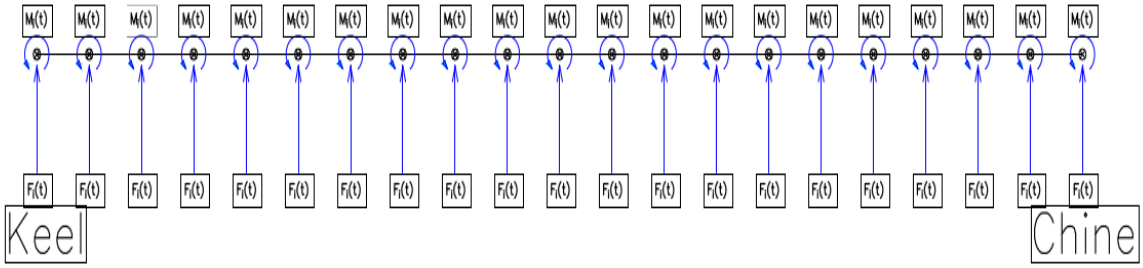

Figure 4.9: Nodal forces and moments

4.9 Time Stepping Technique

Time stepping methods/techniques are algorithms that are used to compute the numerical solution of the ordinary/partial differential equations in varying time. The time stepping technique used here is the Newmark - Beta method as referenced from [17] which is a second order accurate time stepping and computationally stable technique. It is implicit and non-conditionally stable in nature.

Choice of the technique

There are plenty of time stepping techniques available which are of higher order accuracy such as Runge-Kutta fourth order method, Newton-Raphson method, Euler method, etc. However upon analysis it was found that the stiffness quotient of the equation increases unrealistically, the equation becomes unstable and the solution for the equation blows up. It should also be noted that upon reducing the time interval between consecutive time steps still the solution was found to be diverging for all of the above said methods than Newmark-Beta [17] time stepping technique. Hence, this method is chosen.

4.9.1 NEWMARK BETA METHOD

The average constant acceleration scheme with coefficient values γ = 1/2 and β = 1/4 is used. The Newmark-Beta method for direct integration implemented in the program is developed from the following steps:

Initial Calculation

a. Static stiffness matrix [K], mass matrix [M] and damping matrix [C] needs to be formed.

b. Integration parameters such as β and γ needs to be specified for the operation.

c. Integration constants such as b1, b2, b3, b4, b5 and b6 needs to be calculated which will be used

effectively to develop the effective stiffness matrix $\bar{\mathrm{K}}$ = K + b_1M + b_4C.

d. The inverse of the effective stiffness matrix is to be taken and then the initial conditions for the equation are to be specified such as u_0, $\dot{u}_0$, $\ddot{u}_0$.

Each Time Step, t = Δt, 2Δt, 3Δt.....

a. The effective load/force vector for each time step is calculated by :

$$\overline{F}_t \;=\; F_t + M(b_1 u_{t-\Delta t} - b_2 \dot{u}_{t-\Delta t} - b_3 \ddot{u}_{t-\Delta t}) + C(b_4 u_{t-\Delta t} - b_5 \dot{u}_{t-\Delta t} - b_6 \ddot{u}_{t-\Delta t})$$

b. The node displacement vector can be solved at time t by using the triangularization of the inverse matrices by forward and backward substitution as shown in the following equation.

$$[L][D][L]^T u_t = \overline{F}_t$$

c. The node velocities and the accelerations at a time instant t can be calculated by,

$$\dot{u}_t = b_4(u_t - u_{t-\Delta t} + b_5 \dot{u}_{t-\Delta t} + b_6 \ddot{u}_{t-\Delta t}) \Longrightarrow \text{Nodal Velocity}$$
$$\ddot{u}_t = b_1(u_t - u_{t-\Delta t} + b_2 \dot{u}_{t-\Delta t} + b_3 \ddot{u}_{t-\Delta t}) \Longrightarrow \text{Nodal Acceleration}$$

Go back to calculating the effective force vector with each incrementing step.

Chapter 5

SELECTIONS AND REJECTIONS

The above said programming model could not have been achieved without numerous trials and test cases before the working model was finalized. The unsuitable choices were filtered out and in this chapter it is explained in detail as to why the methods, techniques, matrices that were finalized were selected to build this programming model.

5.1 Failure of stiffness matrices

Upon an extensive search for using a pre-defined stiffness matrix, it was found that nearly there were 4 varieties of stiffness matrices that were chosen programmed and tried to build the global stiffness matrix and the governing equation. The four stiffness matrices that were considered were :

- Non - Compatible Preziemiencki Stiffness Matrix
- Compatible Preziemiencki Stiffness Matrix
- Rudolph-Szilard Stiffness Matrix
- Adini-Clough Stiffness Matrix

The local 12x12 non-compatible stiffness matrix developed by Preziemiecki as ref. in [22]

was first programmed into the coding model. It was found that as the matrix was non-compatible to deflection, hence the matrix could not be used to solve for delfections as such.

The compatible Preziemiencki stiffness matrix as ref. in [22] was coded and the tests runs were made for the simple static solution with a ramped-up force varying in time. It came to knowledge that this matrix failed on two different fronts. The first being, the deflection values took long time to converge and that as the mesh sizes kept on increasing as well the solution obtained was not still comparably close to the static solution as well. Even though this was a significant improvement over the previous stiffness matrix, it was decided that if an improvement could be found this could be supplanted with a better one.

Rudolph-Szilard stiffness matrix as ref. from [24] tackled the problem of mesh sizes,in the sense that the even as the mesh sizes became larger and larger still the system of equations were stable and the deflection values were found however it was realized that the deflection values found were not closely comparable with the static solution.

5.2 Selected Stiffness Matrix

The stiffness-matrix based on Adini-Clough finite plate element was referred from [23]. The author had developed a stiffness matrix highly suitable for time dependent phenomenon such as explosion, blasts and it was found really suitable when the same was employed for hull slamming. The difference was that, this stiffness matrix was built in consideration with the nodes and their stiffness parameter along with the joints of the plate elements to the other finite plate elements thereby tacking the conversion of the local to the global matrices.

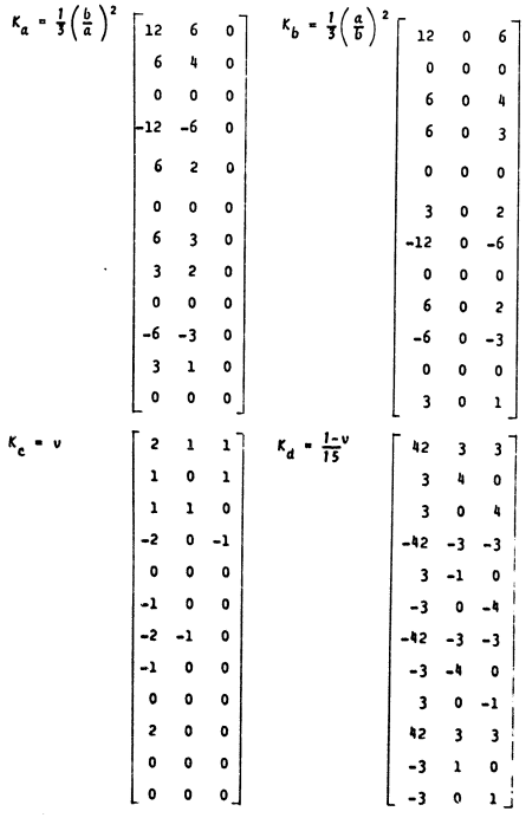

Figure 5.1: Individual stiffness matrices (Ian R.Stubbs,1966)

The sum of the individual stiffness matrices K_a, K_b, K_c and K_d actually give rise to the individual submatrix K_i which arranged to form the 12x12 local stiffness matrix [K] as shown in figure 5.2

5.3 Rejected Numerical Methods

Numerical methods aplenty were coded and tested to solve for the dynamic process but it came to knowledge that only one of the numerical method which could satisfy the conditions were chosen from the lot. The numerical methods that were tested included:

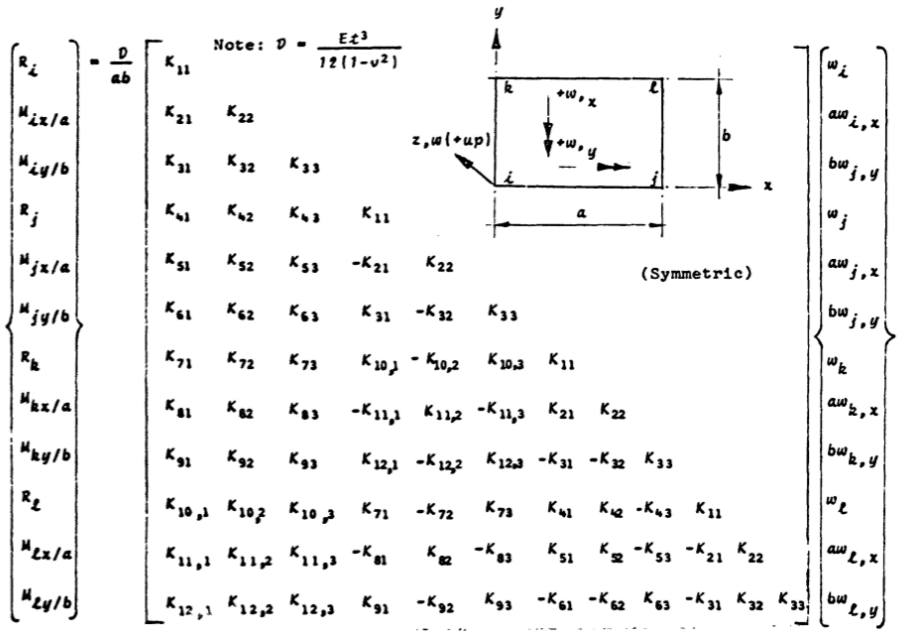

Figure 5.2: The Local Stiffness Matrix based on dynamic response of blasts for box-type structures (Ian R.Stubbs,1966)

- Forward Euler method
- Newton-Raphson method
- Fourth-Order Runge Kutta Method
- Second order-Newmark Beta Method

The forward Euler method was programmed and the system of equations were attempted to be solved by this method. As the method required a great initial value to start with and as well lacked stability, hence the equation grew stiff and the solution started to diverge. Newton-Raphson numerical method was programmed however it was found that the convergence with the static solution lacked stability and hence the solution diverged. The higher-order/fourth order Runge-Kutta method was able to tackle the problem of convergence and it was found that the solution tends to converge however the

detrimental aspect was that the governing equation grew stiff and that the solution lacked stability, hence the solution started to diverge.

5.4 Selected Numerical Method

As referenced from [16], the most suitable method that could provide convergence and retain the stability for a dynamic process such as slamming was the second-order Newmark-beta numerical method. This method was highly stable and the unconditional stability was dependent on the select few coefficients as explained below. This method could provide highly appreciable results and could still retain the stability even if the mesh sizes were to increase to a large number of elements.

I. INITIAL CALCULATION

A. Form static stiffness matrix $\mathbf{K}$, mass matrix $\mathbf{M}$ and damping matrix $\mathbf{C}$

B. Specify integration parameters β and γ

C. Calculate integration constants

$$b_1 = \frac{1}{\beta \Delta t^2} \qquad b_2 = \frac{1}{\beta \Delta t} \qquad b_3 = \beta - \frac{1}{2} \qquad b_4 = \gamma \Delta t b_1$$

$$b_5 = 1 + \gamma \Delta t \; b_2 \qquad b_6 = \Delta t (1 + \gamma b_3 - \gamma)$$

D. Form effective stiffness matrix $\overline{\mathbf{K}} = \mathbf{K} + b_1 \mathbf{M} + b_4 \mathbf{C}$

E. Triangularize effective stiffness matrix $\overline{\mathbf{K}} = \mathbf{L}\mathbf{D}\mathbf{L}^{\mathbf{T}}$

F. Specify initial conditions $\mathbf{u}_0$, $\dot{\mathbf{u}}_0$, $\ddot{\mathbf{u}}_0$

II. FOR EACH TIME STEP $t = \Delta t, \; 2\Delta t, \; 3\Delta t$ ------

A. Calculate effective load vector

$$\overline{\mathbf{F}}_t = \mathbf{F}_t + \mathbf{M}(b_1 \mathbf{u}_{t-\Delta t} - b_2 \dot{\mathbf{u}}_{t-\Delta t} - b_3 \ddot{\mathbf{u}}_{t-\Delta t}) + \mathbf{C}(b_4 \mathbf{u}_{t-\Delta t} - b_5 \dot{\mathbf{u}}_{t-\Delta t} - b_6 \ddot{\mathbf{u}}_{t-\Delta t})$$

B. Solve for node displacement vector at time **t**

$\mathbf{L}\mathbf{D}\mathbf{L}^{\mathrm{T}}\mathbf{u}_t = \overline{\mathbf{F}}_t$ forward and back-substitution only

C. Calculate node velocities and accelerations at time **t**

$$\dot{\mathbf{u}}_t = b_4(\mathbf{u}_t - \mathbf{u}_{t-\Delta t}) + b_5 \dot{\mathbf{u}}_{t-\Delta t} + b_6 \ddot{\mathbf{u}}_{t-\Delta t}$$

$$\ddot{\mathbf{u}}_t = b_1(\mathbf{u}_t - \mathbf{u}_{t-\Delta t}) + b_2 \dot{\mathbf{u}}_{t-\Delta t} + b_3 \ddot{\mathbf{u}}_{t-\Delta t}$$

D. Go to Step II.A with $t = t + \Delta t$

Figure 5.3: Summary of the Newmark numerical method (Newmark, 1959)

Chapter 6

VALIDATIONS

The solution for determining the deflection of a flat plate is evaluated empirically by Roark's Formulas for Stress and Strain [29]. A validation can be performed in the manner that the convergence in deflection could be achieved when the solution is evaluated using many different mesh sizes dynamically.

Roark's Solution : The deflection of the rectangular plate in the Roark's solution is given by the empirical formula based on the boundary conditions. The empirical formulations for rectangular plate with fixed-fixed and simply supported are totally different. The formualations are as following:

6.1 Fixed Supported Boundary Condition

$$y_{max} = \frac{\alpha * q * b^4}{E * t^3} \tag{6.1}$$

where,

α - Coefficient based on the aspect ratio

q - Static Pressure

b - Smaller dimension of the plate

E - Young's modulus

t - Thickness of the plate

a/b	1.0	1.2	1.4	1.6	1.8	2.0	∞
α	0.0138	0.0188	0.0226	0.0251	0.0267	0.0277	0.0284

The above said formulation yields the result y_{max} = 0.06249 mm with α = 0.0284 and q = 0.0003 N/mm^2.

An uniform pressure distribution is acted upon uniformly along the plate surface and the deflection is evaluated for the same. The ramped force distribution is as shown below:

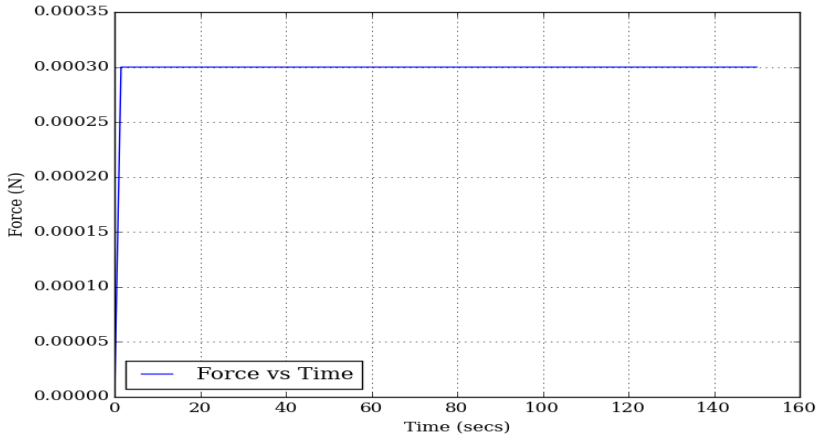

Figure 6.1: Uniform Ramp Force Distribution

6.2 Temporal Convergence

The Newmark-Beta numerical method is included into the existing program for comparing the closed form of [29] with the Newmark solution obtained numerically. The Newmark-Beta scheme provides the scope for understanding the transient solution over a period of time in comparison with the static solution obtained by the Roark's empirical formulation.

A programming model for the static solution is developed and the solution is derived for the

same case where a uniform pressure q = 0.0003 N/mm^2 acts upon the entire plate. The plate is discretized based upon the arbitrary mesh sizes and the Roark's solution is compared to them. The results are shown in table 6.1.

Mesh Size	Newmark Solution	Static Roark Solution
6x6	0.0642	0.06249
8x8	0.0637	0.06249
10x10	0.0633	0.06249
12x12	0.0631	0.06249
14x14	0.0629	0.06249
16x16	0.06287	0.06249
18x18	0.06284	0.06249
20x20	0.0628	0.06249
22x22	0.06274	0.06249
24x24	0.06272	0.06249
26x26	0.06271	0.06249

Table 6.1: Newmark's solution vs Static Roark Solution

The deflection vs time values are plotted one against the other after the above said steady-ramp force is applied to the plate. The plot shows the deflection profile of a central node having the fixed-fixed end conditions. This simulates a steady-state input and the result shows a convergence. The green line shows the static solution as calculated by the Roark formulations. The red line shows the oscillating deflection solution as derived by the Newmark-Beta scheme. The plot is as shown in figure 6.2.

The velocity of the central node is calculated by means of the Newmark-beta method and it is found to be converging as well. The same applies in the case of acceleration of the central node.

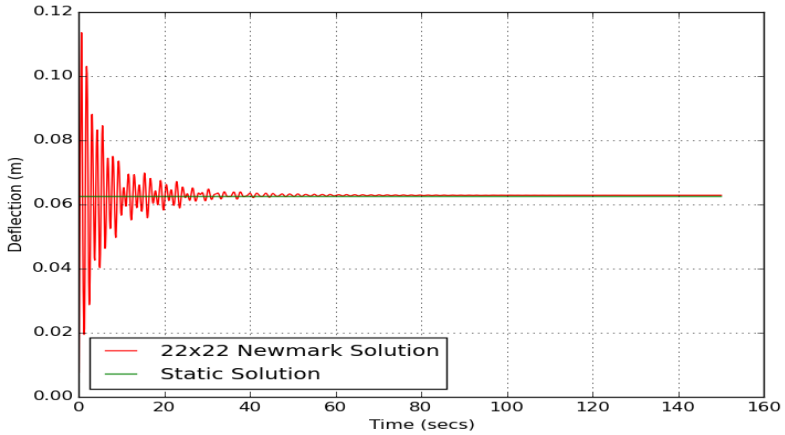

Figure 6.2: Convergence of the Newmark solution with Static Roark solution - Deflection
Fixed - Fixed end plate

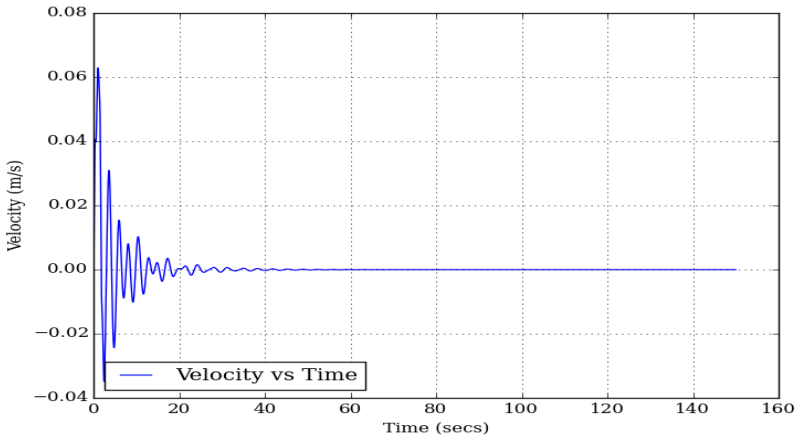

Figure 6.3: Convergence of the Newmark solution with Static Roark solution - Velocity
Fixed - Fixed end plate

The following figures 6.5(a & b) show the convergence of the transient solution with the deflection obtained by the statical solution. The mesh density determines the accuracy of the solution.

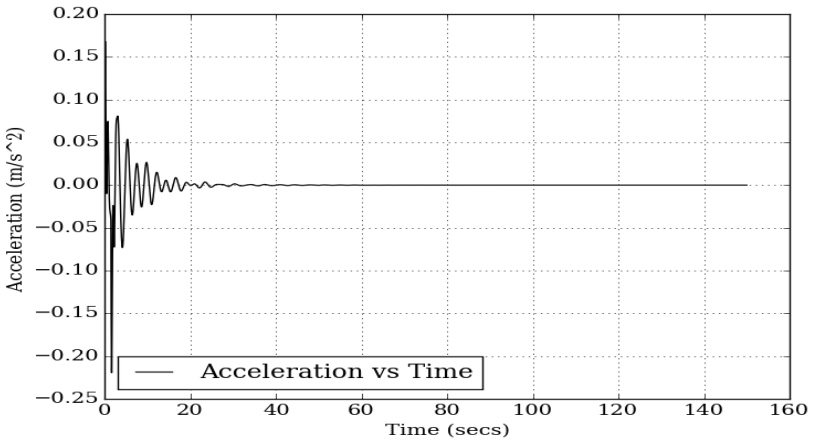

Figure 6.4: Convergence of the Newmark solution with Static Roark solution - Acceleration Fixed - Fixed end plate

6.3 Mesh size - Spatial Convergence

The meshsize is increased in a hierarchial number to achieve better accuracy for the deflection results of the plate. Higher the mesh size, the solution achieves a highly accurate value.

Spatial convergence is attained when there is no change in the accuracy of the solution when the mesh size is increased no matter what. This convergence shows that the solution is appreciable and can be considered for further application. The figure 6.6 shows the spatial convergence.

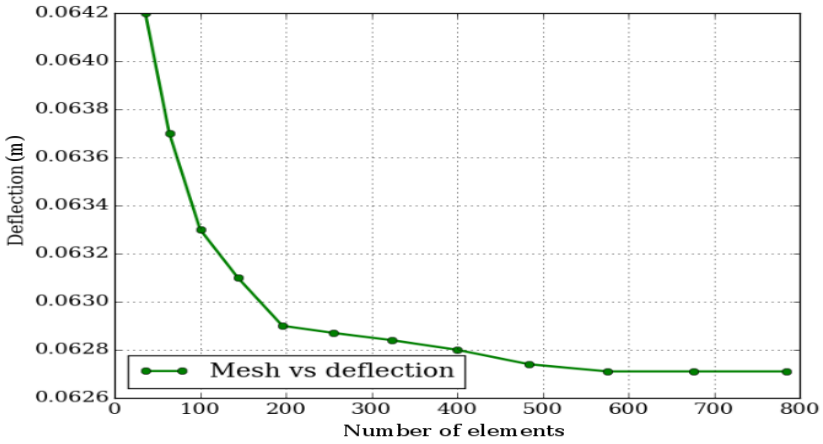

(a) Deflection Convergence

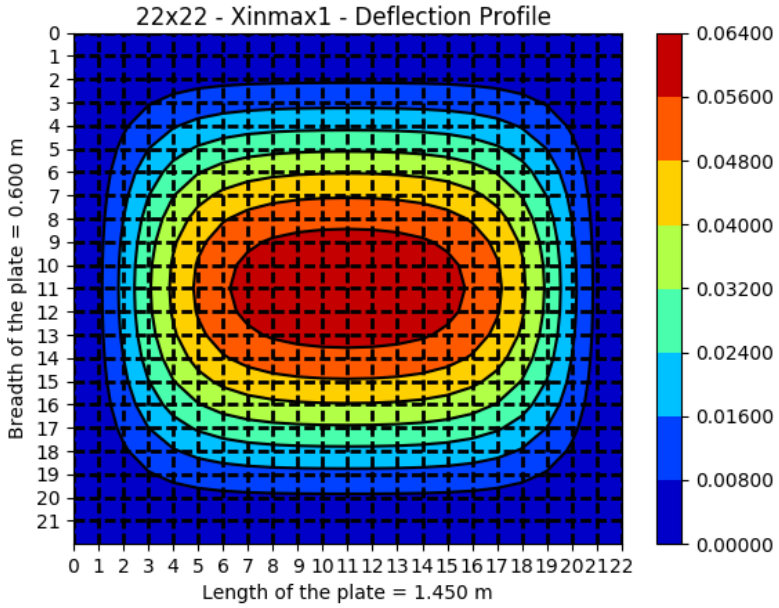

(b) Surface Deflection Contour - Uniform Pressure Distribution

Figure 6.5: Temporal Convergence

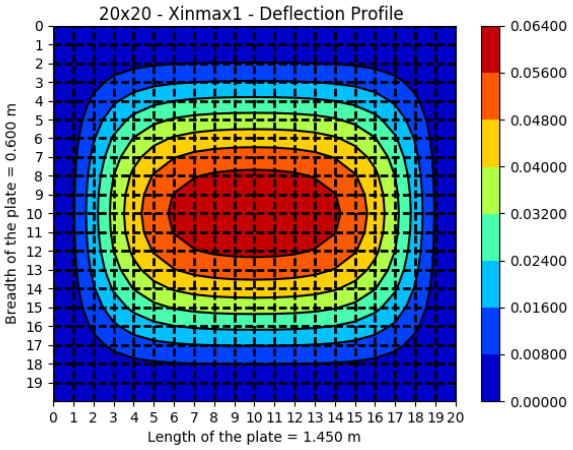

(a) Mesh Size - 20x20 - 400 elements

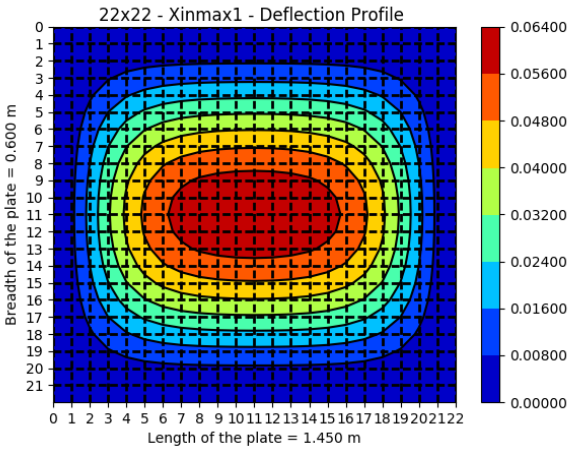

(b) Mesh size - 22x22 - 484 elements

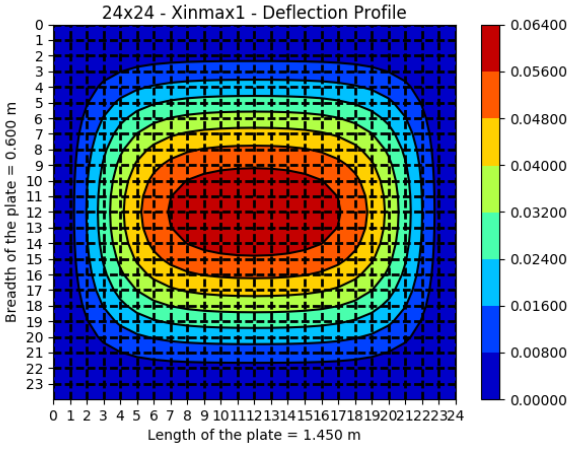

(c) Mesh Size - 24x24 - 576 elements

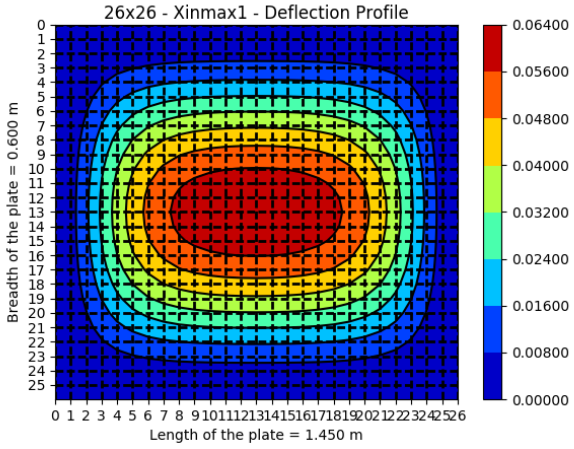

(d) Mesh Size - 26x26 - 676 elements

Figure 6.6: Spatial Convergence

Chapter 7

RESULTS

The analysis was carried out for the wedge shaped hull with the mentioned geometric dimensions. The results from the theoretical predictions and the experimental runs are discussed in this chapter. Spatial and temporal convergence tests are carried out to find out the accuracy and credibility of the solution. The analysis was carried out with different time intervals ΔT = 0.00001 secs, 0.00005 secs and 0.0001 secs. The results were compared and the convergence was evaluated.

The theoretical predictions and the wedge-drop experimental output files were used to compute the deflection of the wedge plate. The surface deflection contours for the above said processes are compared here. There is a comparison of the deflections from either of these processes along with the deflections from the S-DIC (Standard Digital Image Co-relation) technique. The deflection for different plate thicknesses are evaluated and compared as well.

Principal Parameters

The principal parameters of the wedge hull are as follows:

Material	Aluminum
Youngs' Modulus	$69\times10^9\ N/m^2$
Structural damping factor	0.002
Wedge Weight	1153.60 N/m
Bottom plate thickness	0.00635 m
Maximum length	1.450 m
Half-beam	0.60 m
Depth	0.533 m
Deadrise angle	20 $\deg$
Poisson's ratio	0.33

The program was tested for universality and applicability by changing the mesh sizes, time intervals, theoretical and experimental pressure distributions. It has to be noted that spatial convergence requires an appreciable mesh size and temporal convergence is independent of the mesh size. In the theoretical pressure predictions it was found that the process to achieve convergence was computationally intensive and expensive in terms of time and power. In spite of all this, the program was tested with the Newmark-Beta numerical method yielding credible results which are as follows.

The maximum deflection for the theoretical pressure prediction was evaluated to be at 2.8 mm which was achieved to be at a mesh size of 8×8,10×10,12×12 number of elements for the time interval ΔT = 0.0001 secs.

7.1 Tests for Variation and Convergence

Specific tests were carried out on the test case to ascertain the universality of the imposed conditions of nodal forces, added mass, deflection convergence and the like. The tests are shown performed very coherently and their results are displayed to understand the way in which the wedge plate behaves. The wedge model has a vertical drop velocity of 3.05 m/s and all the inputs used for the code are based on this condition.

7.1.1 Time Convergence Test

The program was checked for the application of the external force on the mid node at three different time intervals to investigate the convergence of the force distribution for the wedge plate under fixed-fixed end boundary conditions. The excitation at three different time steps at the mid-node is shown below and the deflection for the same is shown subsequently later.

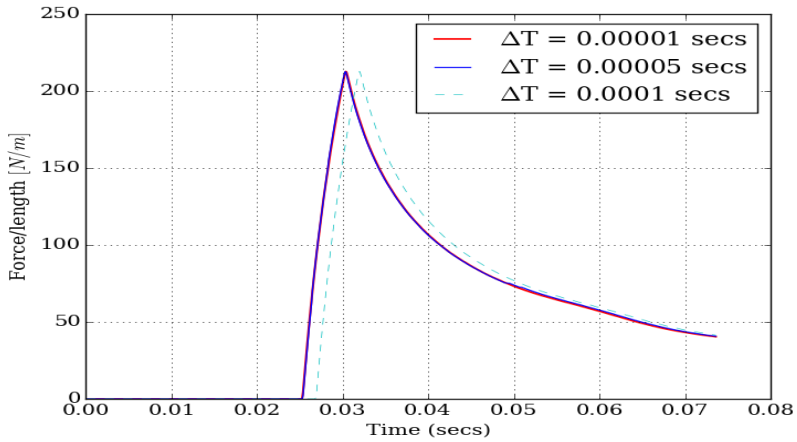

Figure 7.1: Time based convergence for nodal force on the central node of the wedge plate at V = 3.05 m/s across ΔT=0.00001,0.00005 and 0.0001 secs - Theoretical Pressure Predictions

The above plot actually shows that the application of forces are still stable even during different

time steps. The stability of the system under investigation holds stead and the plot also shows that the transient nature of the solution can be studied. The transient solutions were very well captured for the above said timesteps, indicating the non-conditional stability of the Newmark-Beta numerical method. The excitation force values mostly overlap through the time range across varied time intervals as seen.

This restraint holds good for the experimental wedge drop as well and the evaluation of an imposed force on a central node is shown as in figure 7.2.

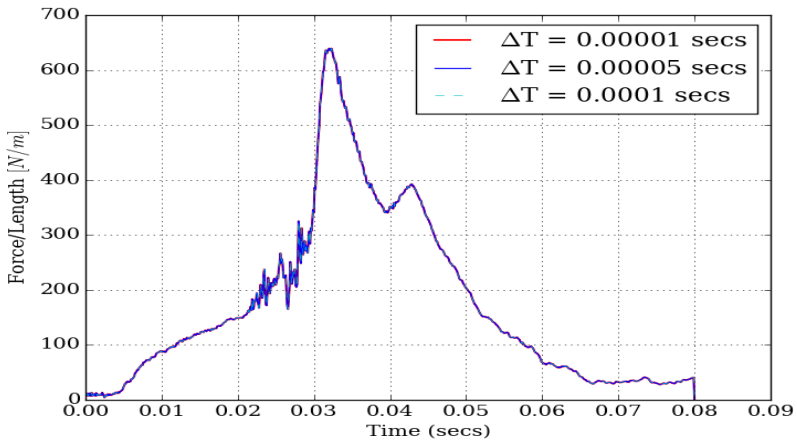

Figure 7.2: Time based convergence for nodal force on the central node of the wedge plate at V = 2.94 m/s across ΔT=0.00001,0.00005 and 0.0001 secs - Experimental wedge drop results

Added mass when compared across the three time steps also was found to obey convergence thereby reiterating the universality of this technique.

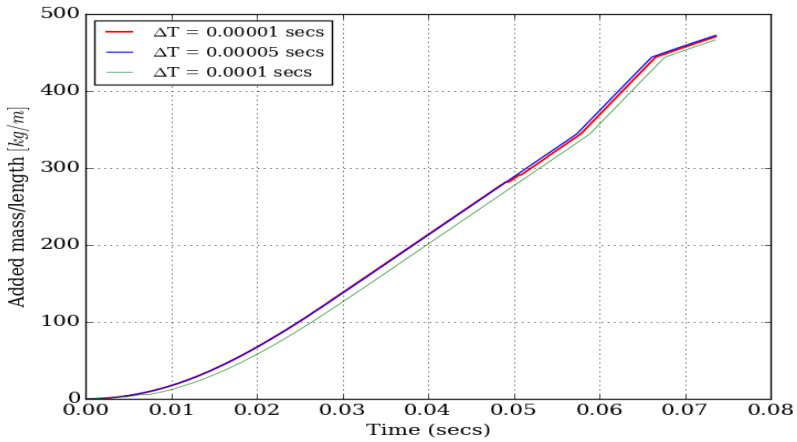

Figure 7.3: Time based convergence for added masses on the wedge plate at V = 3.05 m/s across ΔT=0.00001,0.00005 and 0.0001 secs - Theoretical Pressure Predictions

7.1.2 Pressure Distribution

The theoretical and experimental pressure distribution which yields the maximum deflection is compared as shown below. The experimental pressures were measured at 8 distinct locations along the bottom plate from the keel to chine. The pressures were measured discreetly and under credible assumption it was developed into a distribution on the basis that the pressure measured at location 1 will be the same along the half of the distance between 1 and 2. Based on this assumption, the step like pressure distribution was developed taking into account the pressures being measured at all the discrete locations.

The deflection was maximum at t = 0.0183 $secs$ in case of theoretical pressure distribution and at t = 0.0227 $secs$ in case of experimental pressure distribution. The following plot shows that even though the wetted length at t = 0.0183 $secs$ is very less, the maximum pressure value touches nearly 60000 N/m^2 as against the experimental pressure distribution which experiences a maximum instantaneous pressure of nearly 47000 N/m^2 when the pressure is measured at 8 different locations by the use of pressure transducers from keel to chine.

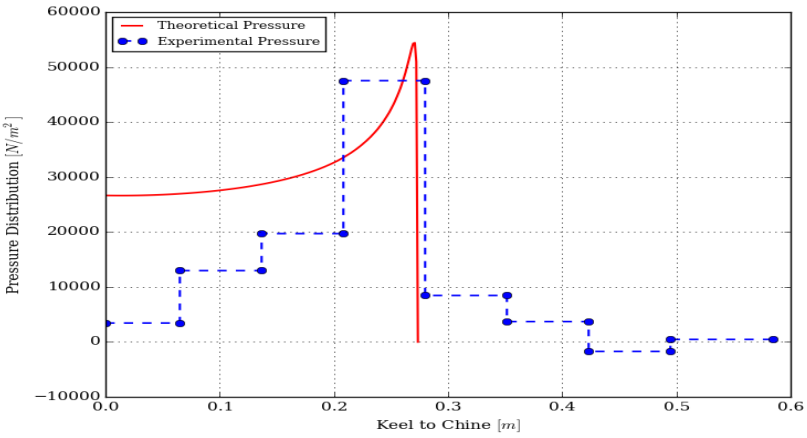

Figure 7.4: Pressure distributions - Theoretical vs Experimental-Peak pressure time instants

7.1.3 Deflection Convergence Test

The deflection is evaluated at the central node for the theoretical pressure prediction distribution output and the experimental wedge-drop runs.

Deflection Convergence - Theoretical Pressure Prediction

The mid-node experiences maximum deflection at a particular time step and this is evaluated for different time intervals ΔT = 0.00001, 0.00005 and 0.0001 secs. The accuracy of the solution is improved as the number of mesh elements are continuously increased till it reaches the maximum deflection value. Ideally, the whole deflection pattern of the central node should have converged/followed the same pattern, however even after a very appreciable mesh size it was found that only the maximum deflection converged and that the pattern didn't observe convergence.

The reason being that the pressures, wetted lengths and forces measured from the output file seemed to be very fine nearly to the point of $5/6^{th}$, hence the time and the effort for computation and running the program was quite long. This actually slowed down the progress of evaluating the results and it was decided that the trial runs can be stalled when the mesh size reached 26x26 elements, since the

dynamic test solution converged well enough at that point.

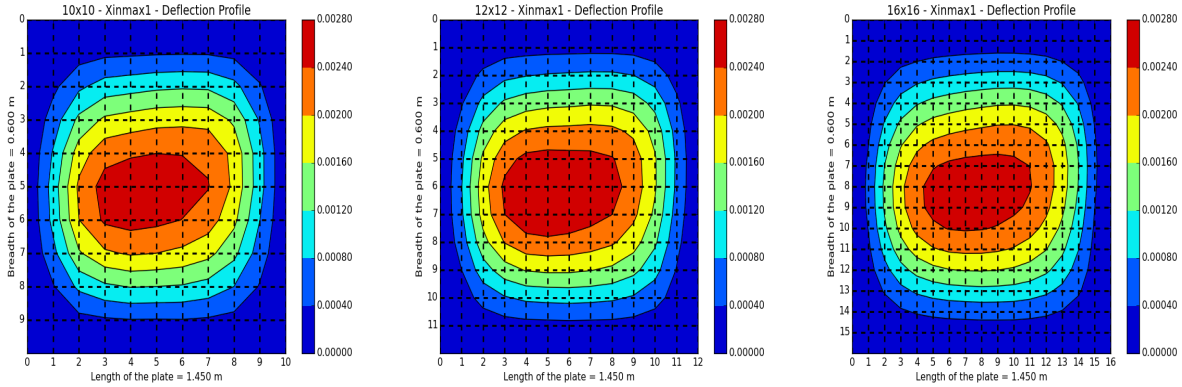

(a) 10x10-Mesh elements (b) 12x12-Mesh elements (c) 16x16-Mesh elements

Figure 7.5: Max. deflection convergence surface contour - Experimental Pressure distributions-ΔT=0.0001 secs

Deflection Convergence - Experimental Wedge drop

The deflection convergence pattern and contour of the mid node for the rectangular wedge plate under fixed-fixed end condition is evaluated. Upon analysis it is found that the maximum deflection occurs at a particular time step for all different mesh sizes and time intervals, the deflection convergence pattern is observed as well. The maximum deflection is of $2mm$. This is considered to be an adequate value since the maximum deflection observed during the wedge drop experiment under different boundary conditions from the pinned-pinned at the keel and fixed-fixed at the chine with a test velocity of v=2.94 m/s, for a 0.6096 m (24 $inch$) drop-height wedge-drop experiment yields δ = 0.125 $inch \approxeq$ 3.175 mm.

As the bottom plate panel under study is considered to be fixed-fixed, the deflection is much more lesser than the experimental wedge-drop case. The deflection of the central node and the surface contour at the maximum time instant is shown in figure 7.7.

The max.deflection values for ΔT = 0.00001, 0.00005 and 0.0001 secs was found to be at

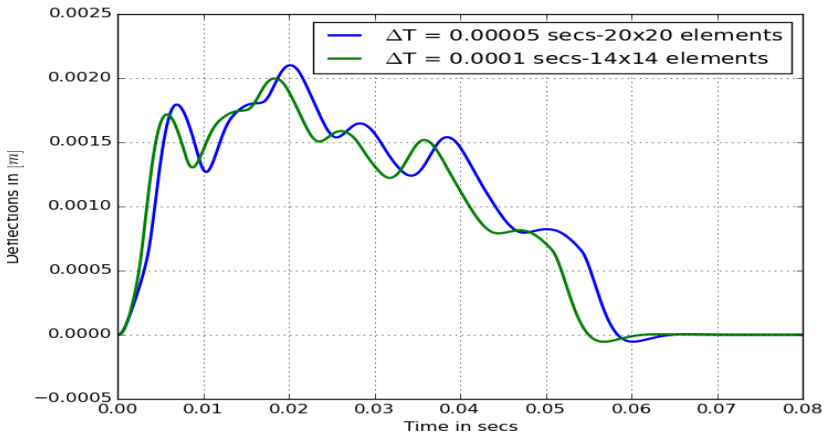

Figure 7.6: Convergence of deflection of the mid-node varying in different time intervals ΔT=0.00005 and 0.0001 secs with different mesh sizes - Experimental Wedge Drop results.

t=0.00183 *secs* for the above said three runs.

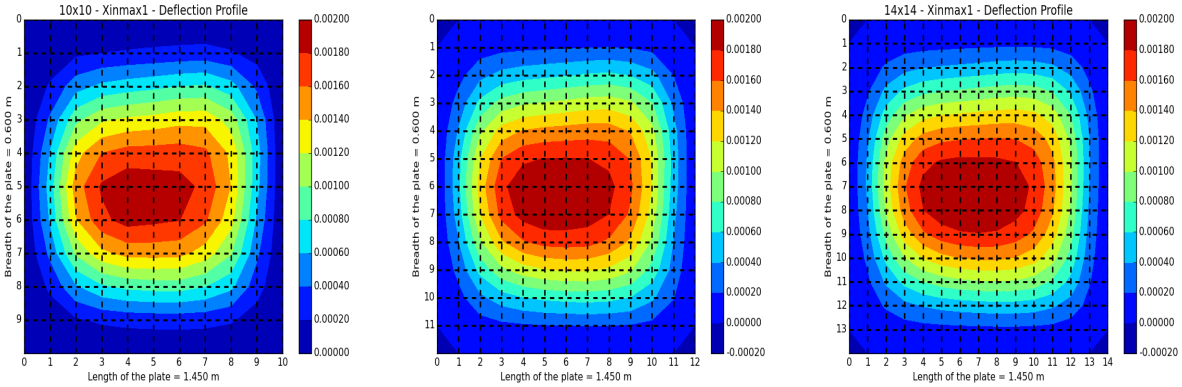

(a) 10x10-Mesh elements-ΔT=0.0001 secs

(b) 12x12-Mesh elements-ΔT=0.0001 secs

(c) 14x14-Mesh elements-ΔT=0.0001 secs

Figure 7.7: Max. deflection convergence surface contour - Experimental Pressure distributions-ΔT=0.0001 secs

The convergence for mesh sizes and no. of elements is evaluated and it was observed that the maximum deflection was occurring at the same time instant t=0.0192 secs for all the mesh sizes in

addition to the deflection profile pattern of the different number of mesh elements as seen in figure 7.9

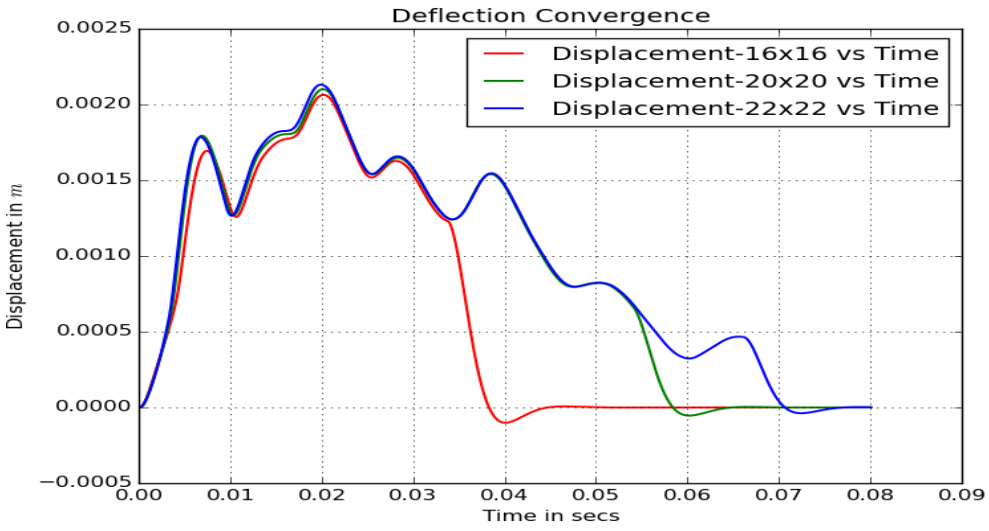

Figure 7.8: The deflection convergence of the various mesh sizes with the same $\Delta T = 0.0001$ secs - Experimental Pressure Distributions

7.2 Panel deflections

The deflection of the wedge plate during the time of wedge-drop being tested for various velocities and boundary conditions is explained below. This provides a very hollistic and erudite manner of the presentation of the whole process and the deflection of the bottom plate.

The deflection profile experiences a steady peak and hits the maximum at ts = 0.00183 secs and then starts to waywardly follow the path and damps down irregularly, goes to a minimum at about t = 0.06 secs in a complete range of t = 0.08 secs.

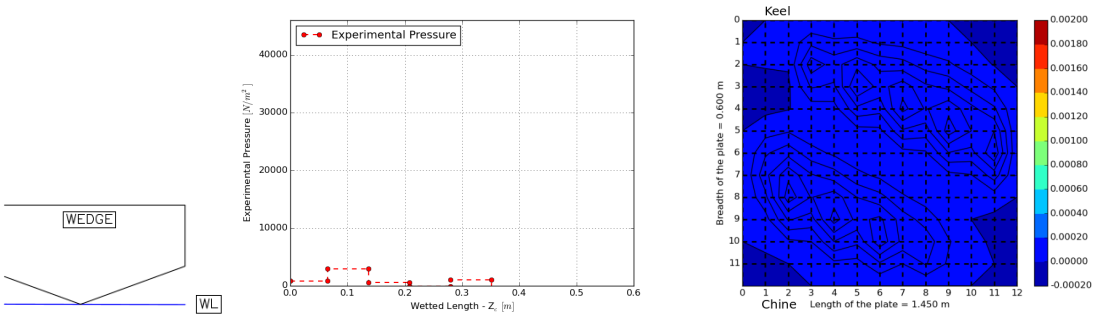

Figure 7.9: Experimental pressure distribution and wedge panel deflection for t=0.0002 secs

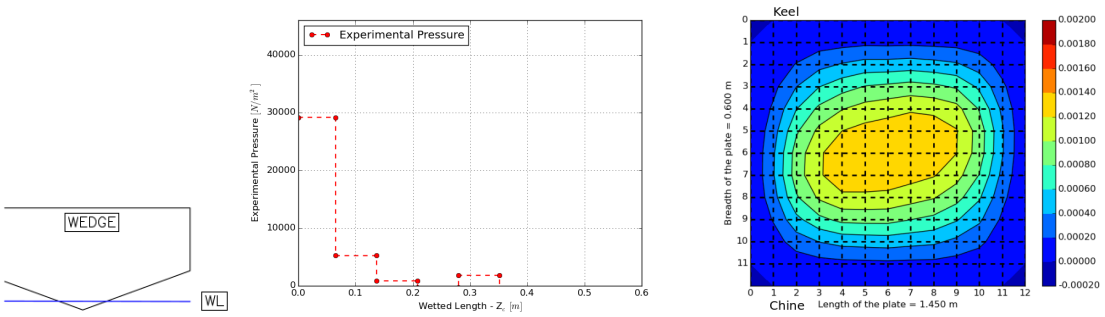

Figure 7.10: Experimental pressure distribution and wedge panel deflection for t=0.0049 secs

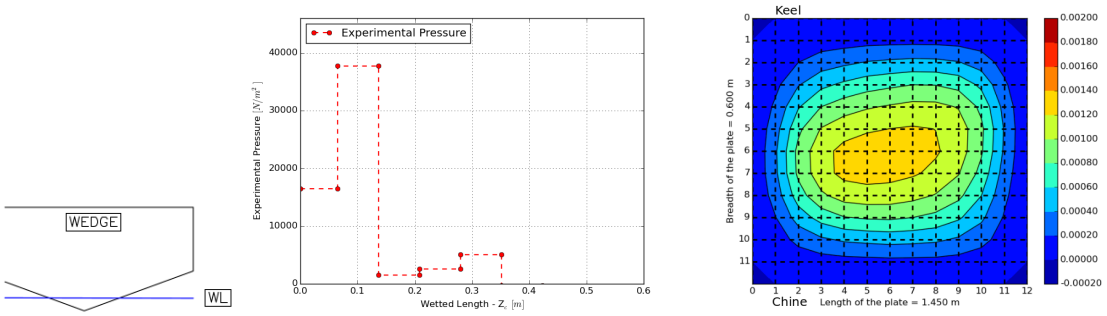

Figure 7.11: Experimental pressure distribution and wedge panel deflection for t=0.0099 secs

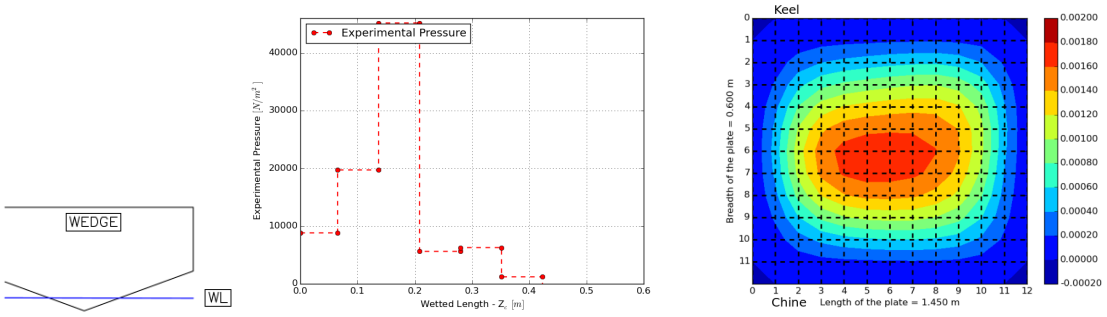

Figure 7.12: Experimental pressure distribution and wedge panel deflection for t=0.0149 secs

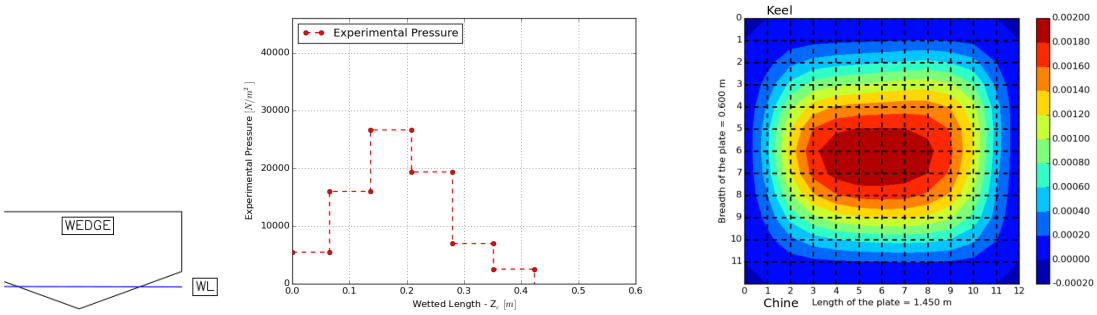

Figure 7.13: Experimental pressure distribution and wedge panel maximum deflection for t=0.0182 secs

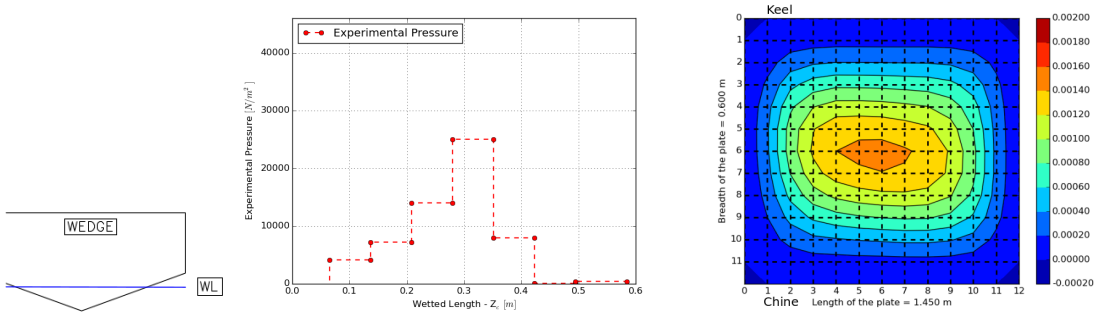

Figure 7.14: Experimental pressure distribution and wedge panel deflection for t=0.0349 secs

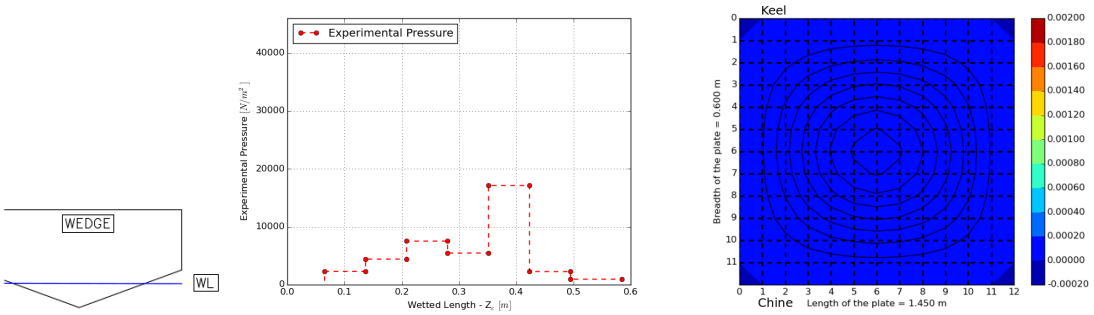

Figure 7.15: Experimental pressure distribution and wedge panel deflection for t=0.0499 secs

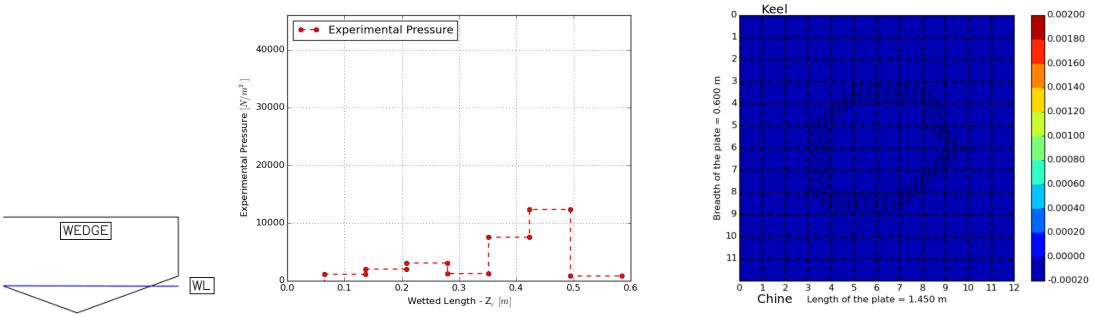

Figure 7.16: Experimental pressure distribution and wedge panel deflection for t=0.0599 secs

The above shown surface contour plots illustrate the deflection profile of the bottom wedge plate under slamming taken over a range of 0.08 secs for the experimental pressure distributions with time interval $\Delta T = 0.0001$ secs.

7.3 Plate deflection symmetry

It was observed that the plate deflection at a particular time step in the time range was observed to be asymmetrical instead of the anticipated symmetrical deflection pattern. Numerous tests varying the mesh sizes, the added masses formulation, the loading force vector, stiffness matrices, mass ma-

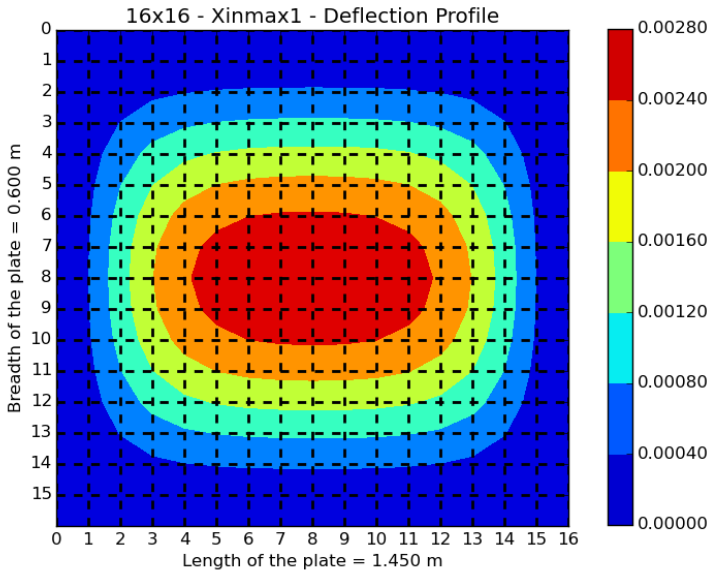

Figure 7.17: Symmetrical Plate Deflection - Force vector distributed transversely throughout the plate

trices etc. were conducted to find out the root cause behind this. After numerous practical attempts it was decided to forcibly simulate a uniformly distributed force vector ranging entirely over the transverse width(complete wetting of the nodes) of the plate compared to the partial wetting of the nodes, as seen from the input file generated from the wedge drop experiment.

The results of this test proved that the symmetrical deflection as visible in figure 7.17, was observed as opposed to the asymmetrical deflection pattern observed previously as in figure 7.18, when the nodes were partially wetted. As the plate nodes are partially wetted, it means that at a certain time instant the pressure distribution does not act entirely on the transverse width of the plate, rather only till an arbitrary point ie., the force vector becomes zero after that point till the end of the plate nodes. This reason was attributed to the asymmetrical deflection as this seemed to be the most appreciable reason that could validate this occurrence.

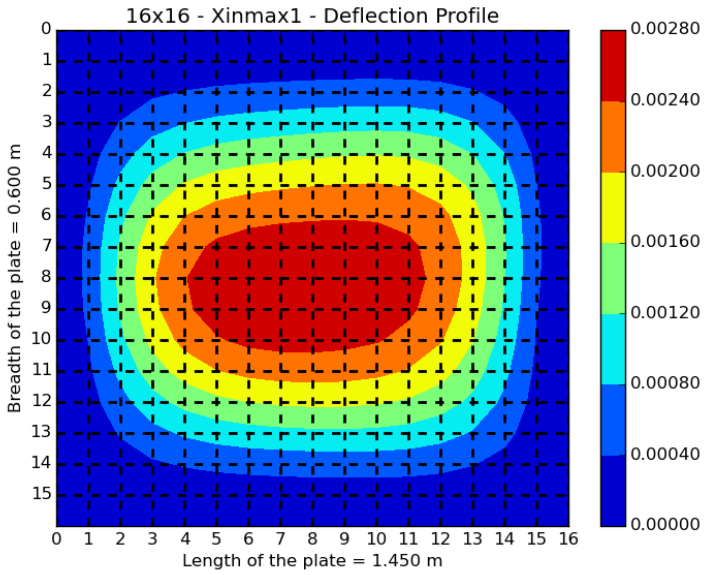

Figure 7.18: Asymmetrical Plate Deflection - Force vector not occurring transversely throughout the plate

7.4 Thickness variation test

The deflection was computed for three different wedge plate thicknesses which was : 3.175mm, 4.7265mm and 6.35mm. The default thickness of the plate was 6.35mm and until now all the results were based on that. As the plate thicknesses were reduced, larger deflections were expected as the flexural rigidity of the plate depends on the cubic factor of the thickness of the plate.

$$D = \frac{E * h^3}{12 * (1 - \nu^2)} \tag{7.1}$$

where, E - Youngs' Modulus, h - plate thickness and ν - Poisson's ratio

The flexural rigidity is directly related to the plate thickness, which implies that as per our expectation the deflection will be more when the plate thickness is less. A plot of fixed-fixed plate with different plate thicknesses showing the maximum deflection is shown below.

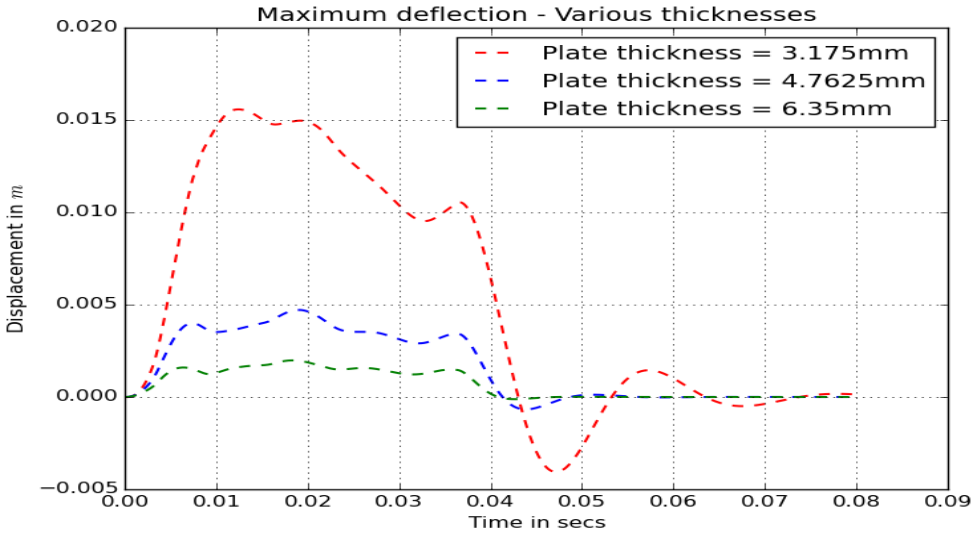

Figure 7.19: Maximum Deflection of fixed-fixed plate with fixed-fixed end conditions for ΔT=0.0001 secs

As expected for a rectangular plate with thickness t = 6.35 mm , the maximum deflection was computed to be δ = 2 mm, however when tested for t = 4.7625 mm the maximum deflection was computed be around δ = 4.5mm and for t = 3.175 mm it resulted in δ = 15 mm.

This shows that the thickness of the plate can significantly affect the deflection profile of the plate.

S No.	Plate Thickness(mm)	Deflection(mm)
1	3.175	15.027
2	4.7625	4.533
3	6.350	2.012

Table 7.1: Wedge Plate Deflections for various plate thicknesses

There seems to be a 86.6 % and a 55.6 % deviation in the deflection results of t=3.175 mm, t=4.7625 mm when compared with base plate thickness t=6.350 mm. This is quite a significant

deviation and has to be noted that just the change in plate thickness alone influences this deviation.

7.5 Deflection Comparisons-Theoretical,Experimental and S-DIC

S-DIC or Stereoscopic Digital Image correlation is a contact-free method for measuring the surface strain and deformation experienced by a material under stress. It works by analyzing variations in a series of images taken from a fixed location and is most suitable for flat, planar surfaces. The S-DIC technique utilizes two cameras for stereovision. These cameras must be calibrated to perform the triangulation of points. By calibration it means that the focal length of the camera and its positioned needs to be fixed and regulated. This inturn helps for performing the triangulation of points in space to determine the deflection of the plate.

The deflection response of the bottom wedge plate measured by strain gauges during the wedge drop experimental procedure, the response derived by utilizing the output of the theoretical pressure prediction and the results from the S-DIC (Stereoscopic Digital Image Correlation) are compared to find out the deflection results of the bottom plate and the optimum is chosen. The comparison between the responses of the three techniques are shown below:

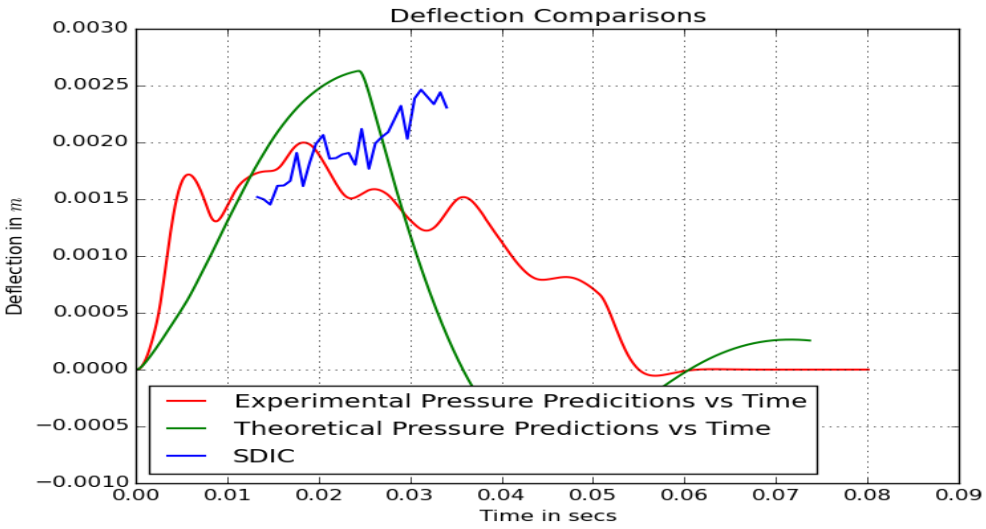

Figure 7.20: Deflection Comparisons

As shown in figure 7.18, it can be understood that we get different maximum values of deflection when the responses from different inputs were compared and evaluated. Upon analysis it was found that, the maximum peak value from experimental pressures was found to be $2mm$ when compared to theoretical pressures which yielded $2.6mm$ and response from SDIC which resulted in $2.5mm$. There seems to be a 20% deviation in the maximum deflection from SDIC and a 24% deviation in the maximum deflection from theoretical pressures as compared against the experimental pressure response.

Chapter 8

CONCLUSIONS

A FORTRAN 90 program has been developed to predict the deflection of the wedge plate by theoretical pressure prediction methods by making use of the dynamic numerical time-integration methods like the Second Order Newmark-Beta method. Various tests have been performed to validate the accuracy, stability, applicability and the universality of the output solution.

The program was tested for three different time intervals ΔT = 0.00001, 0.00005 and 0.0001 secs. The program was tested for an arbitrary mesh size tending to the order of maximum being 28x28 mesh elements for theoretical pressure prediction outputs. The program runs were expensive in terms of effort, time and computational capabilities. However, the results from the theoretical pressure distribution were found to be in convergence at the maximum deflection yielding δ = 2.8mm, however the pattern didn't converge for ΔT = 0.00001 secs. When tested for the time intervals ΔT = 0.00005 and 0.0001 secs, the solutions were found more convergent than the previous time step. It was realized that as the time interval becomes really small there is an issue of convergence as the equation becomes stiff.

The program was validated with a simple Newmark-beta dynamic solution. The solution was checked for convergence with the static solution for validation. The principal problem for the thesis work is solved by providing an output as input from the hydrodynamic code which had pressure distribution generated from the theoretical pressure predictions. In addition to this, the output pressures

recorded from the wedge-drop experiment measured by strain gauges and the S-DIC(Stereoscopic Digital Image Co-relation) are used for comparing and contrasting with the above said methods.

The nodal forces are evaluated for the entire process, in all the above said methods. The deflection profiles and the responses from the above said methods are compared to in the results chapter of this thesis work. The deflection for three different thicknesses were evaluated and it was found that as the plate becomes lighter the deflection becomes higher as expected.

The program developed can actually be used to study the hydroelastic nature of the bottom wedge plate and to estimate the maximum deflection suffered by the plate panel during bottom slamming. The time interval for the test process has to selected cautiously as this can influence the equation to become stiff and thereby suffer a numerical breakdown as well. However, as Newmark - Beta is non-conditionally stable this happens seldom but still care has to be taken in this regard as the time and effort for the computational process depends on this as well.

8.1 Limitations and shortcomings

The shortcoming of this thesis work was that, despite innumerable attempts, it proved futile as the simply supported end conditions could not be realized in contrast to the fixed-fixed end conditions.

It was understood later after the whole trial run that, there seems to be an unknown relationship between the mesh size of the plate and the time interval. This fell beyond the scope of the current thesis work and was left partly explored. The time and effort spent on the same was not significant enough though.

The scope of the thesis work restricted itself to N$\times$N mesh sizes, whereas M$\times$N mesh sizes was remotely explored since time, computational effort became a constraint. The computational time can be reduced by using Iterative method solver such as QR decomposition or LU decomposition in order to solve AX=B, as opposed to the currently used Doo-Little method or the Gauss-Jordan elimination technique. As the mass matrix is sparsely populated effective numerical methods that are precisely

efficient in solving sparsely populated matrices can be used to solve the system of equations much quicker perhaps.

8.2 Future Work

Further analysis can be performed by incorporating or simulating the simply-supported boundary conditions to understand the deflection behavior of the plate. In addition to this the wedge plate can be made of a different composite material as well and can be evaluated for the response.

It was found in the experimental wedge-drop that for all practical purposes even as the bottom plate is considered fixed, that was not the case to be. The portion of the plate near the keel deflects as well and this condition needs to be included in the boundary conditions for the same.

Bibliography

[1] JL Armand and R Cointe. Hydrodynamic impact analysis of a cylinder. *Journal of offshore mechanics and Arctic engineering*, 109(3):237–243, 1987.

[2] Richard ED Bishop and William Geraint Price. *Hydroelasticity of ships*. Cambridge University Press, 1979.

[3] Sheng-Lun Chuang. Experiments on flat-bottom slamming. *Journal of Ship Research*, 10(1):10–27, 1966.

[4] Nabanita Datta. *Hydroelastic response of marine structures to impact-induced vibrations*. University of Michigan, 2010.

[5] ZN Dobrovol'Skaya. On some problems of similarity flow of fluid with a free surface. *Journal of Fluid Mechanics*, 36(4):805–829, 1969.

[6] Jonathan R Eastridge. An experimental study in the hydroelastic response of an aluminum wedge in drop tests. *University of New Orleans Theses and Dissertations*, Vol.2317, 2017.

[7] E Fontaine and R Cointe. A second-order solution for the wedge entry with small deadrise angle. In *Proceedings of the 7th International Workshop on Water Waves and Floating Bodies, Val de Rueil, France*, pages 105–108, 1992.

[8] C Guedes Soares. Transient response of ship hulls to wave impact. *International shipbuilding progress*, 36(406):137–156, 1989.

[9] EM Haugen and O Faltinsen. Theoretical studies of wetdeck slamming and comparisons with full scale measurements. In *FAST. Proceedings of the 5th International Conference on Fast Sea Transportation. USA: FAST*, 1999.

[10] GK Kapsenberg. Slamming of ships: where are we now? *Philosophical Transactions of the Royal Society of London A: Mathematical, Physical and Engineering Sciences*, 369(1947):2892–2919, 2011.

[11] GK Kapsenberg. Slamming of ships: where are we now? *Philosophical Transactions of the Royal Society of London A: Mathematical, Physical and Engineering Sciences*, 369(1947):2892–2919, 2011.

[12] Von Karman. The impact of seaplane floats during landing. *National Advisory Committee for Aeronautics*, Technical Note No.321, October,1929.

[13] AA Korobkin. Three-dimensional nonlinear theory of water impact. In *18th International Congress of Mechanical Engineering (COBEM), Ouro Preto, Minas Gerais, Brazil*, 2005.

[14] Naresh Kumar Koyyapu. Numerical computation of transient response of 2d wedge impact. *University of New Orleans Theses and Dissertations*, Vol.2260, 2016.

[15] CH Lu, YS He, and GX Wu. Coupled analysis of nonlinear interaction between fluid and structure during impact. *Journal of fluids and structures*, 14(1):127–146, 2000.

[16] Jian Lv and Joachim L Grenestedt. Some analytical results for the initial phase of bottom slamming. *Marine Structures*, 34:88–104, 2013.

[17] Nathan M Newmark. A method of computation for structural dynamics. *Journal of the engineering mechanics division*, 85(3):67–94, 1959.

[18] Wilhelm Pabst. Theory of landing impact of seaplanes.

[19] Riccardo Pancirolia and Giangiacomo Minaka. Hydroelastic slamming of composite plates.

[20] Bernard Peseux, Laurent Gornet, and Bundy Donguy. Hydrodynamic impact: Numerical and experimental investigations. *Journal of Fluids and Structures*, 21(3):277–303, 2005.

[21] Dominic J Piro and Kevin J Maki. Hydroelastic wedge entry and exit. In *11th International Conference on Fast Sea Transport. Honolulu, Hawaii, USA*, 2011.

[22] Janusz S Przemieniecki. *Theory of matrix structural analysis*. Courier Corporation, 1985.

[23] Ian R Stubbs and KL Benuska. A computer program for the dynamic blast response of box-type structures. Technical report, LIN (TY) AND ASSOCIATES VAN NUYS CA, 1966.

[24] Rudolph Szilard. *Theories and applications of plate analysis: classical numerical and engineering methods*. John Wiley & Sons, 2004.

[25] Brandon M Taravella and William S Vorus. A general solution to low-aspect-ratio flat-ship theory. *Journal of Engineering Mathematics*, 71(2):171–184, 2011.

[26] William S Vorus. A flat cylinder theory for vessel impact and steady planing resistance. *Journal of ship research*, 40(2):89–106, 1996.

[27] Herbert Wagner. Phenomena associated with impacts and sliding on liquid surfaces. *Z. Angew. Math. Mech*, 12(4):193–215, 1932.

[28] El-Mahdi Yettou, Alain Desrochers, and Yvan Champoux. Experimental study on the water impact of a symmetrical wedge. *Fluid Dynamics Research*, 38(1):47–66, 2006.

[29] Warren Clarence Young and Richard Gordon Budynas. *Roark's formulas for stress and strain*, volume 7. McGraw-Hill New York, 2002.

[30] R Zhao, O Faltinsen, and J Aarsnes. Water entry of arbitrary two-dimensional sections with and without flow separation. In *Proceedings of the 21st symposium on naval hydrodynamics*, pages 408–423. Trondheim, Norway, National Academy Press, Washington, DC, USA, 1996.

Vita

The author Mallikarjun Kalluru has a Bachelors of Engineering in Naval Architecture and Offshore Engineering from Chennai,India. He had worked as a Design Engineer at Pipavav Defence and Offshore Engineering Company Ltd., currently called Reliance Defence Engineering, Gujarat, India.

In his second job, he had worked as a Scientist - B (Research and Design) at Indian Maritime University, Vizag, India. The author is currently doing his Masters in Naval Architecture and Marine Engineering at University of New Orleans, New Orleans.